Check for updates

Received: 8 September 2021 | Revised: 1 February 2022 | Accepted: 2 February 2022

DOI: 10.1002/dep2.184

The Depositional Record Open Access
A journal of the International Association of Sedimentologists
WILEY

ORIGINAL ARTICLE

Depth-limiting resistant layers restrict dimensions and positions of estuarine channels and bars

Harm Jan Pierik[1] | **Jasper R. F. W. Leuven**[1,2,3] | **Freek S. Busschers**[4] | **Marc P. Hijma**[5] | **Maarten G. Kleinhans**[1]

[1]Department of Physical Geography, Faculty of Geosciences, Utrecht University, Utrecht, The Netherlands

[2]Royal HaskoningDHV, Nijmegen, The Netherlands

[3]Department of Environmental Sciences, Hydrology and Quantitative Water Management, Wageningen University, Wageningen, the Netherlands

[4]TNO Geological Survey of the Netherlands, Utrecht, The Netherlands

[5]Department Applied Geology and Geophysics, Deltares, Utrecht, The Netherlands

Correspondence
Harm Jan Pierik, currently at Cultural Heritage Agency of the Netherlands.
Email: hj.pierik@cultureelerfgoed.nl

Funding information
Rijkswaterstaat, Grant/Award Number: 31126483; NWO TTW, Grant/Award Number: 016.140.316/13710

Abstract

Estuaries comprise channels vital for economic activity and bars as valuable habitats. They are increasingly under human-induced pressures (e.g. sea-level rise and dredging), resulting in morphological changes that affect navigability, flood safety and ecology. Antecedent geology may strongly steer how estuary channels will adapt to these pressures, but is surprisingly absent in most models. Here geological data and a unique bathymetry dataset covering 200 years from the Ems-Dollard estuary (Netherlands/Germany) were used to demonstrate how local resistant layers force the position and dimensions of confluences and bars on the scale of an entire estuary. These layers limit channel depth and consequently cause widening, resulting in mid-channel bar formation and increased channel curvature. This could lead to unexpected estuary widening and may cause land loss in densely populated areas. With increasing channel volume (as may happen again under future sea-level rise), resistant layers in the estuary's substrate become more exposed, which enhances their effects. Many systems around the world contain shallow resistant layers that potentially constrain estuary channel dimensions and steer bank erosion. This highlights that resistant layer effects are important to consider as part of mixed depositional processes in coastal environments. It is therefore necessary to globally account for the effects of inherited resistant layers in the possible response of estuaries to sea-level rise and increased tidal penetration.

KEYWORDS

antecedent geology, channel-bar pattern, estuary, Holocene

1 | INTRODUCTION

Estuaries are highly dynamic wetland areas that develop at the transition from the river to the sea. The channels of many large estuaries provide access to harbours (De Vriend et al., 2011) and their intertidal bars are valuable ecological habitats (Bouma et al., 2005; Chen et al., 2016). Estuarine landscapes are formed by processes of sediment transport, mixing and sorting of sand and mud driven by river flow, tidal currents, waves and salinity gradients

This is an open access article under the terms of the Creative Commons Attribution License, which permits use, distribution and reproduction in any medium, provided the original work is properly cited.
© 2022 The Authors. *The Depositional Record* published by John Wiley & Sons Ltd on behalf of International Association of Sedimentologists

(Coco et al., 2013; Dalrymple et al., 1992; Leuven et al., 2016; Townend, 2012), as well as by bioturbation and biofixation of sediments by microphytobenthos, macrobenthos and plant species (Braat et al., 2017; Brückner et al., 2020). Estuaries are increasingly under pressure by human influence mainly resulting from dredging (Essink, 1999; van Maren et al., 2015), sediment depletion (Wang et al., 2016), bank stabilisation (Mosselman et al., 2000) and sea-level rise (Kirwan & Megonigal, 2013; Nicholls & Cazenave, 2010), which potentially cause bottom erosion (Hoitink et al., 2017; Huismans et al., 2016, 2021; Sloff et al., 2013), and may change tidal prism, water levels, channel volume (water volume in the channels below MSL) and bar area (Leuven et al., 2018a).

Besides being driven by hydrodynamical boundary conditions from both the sea and the river, such changes are expected to be strongly steered by resistant layers present in the estuary substrate, such as bedrock, consolidated peat or stiff pre-Holocene clays and tills, which potentially limit channel incision or lateral migration. Such layers are inherited from antecedent geological processes, often not directly related to the present tidal system. Few studies, however, consider these effects on the scale of the entire estuary in the light of future global change (Townend, 2012). Instead, many recent studies on relationships between hydrodynamics and large-scale channel-bar patterns implicitly assume that the estuary subsurface consists of cohesionless sediment and hence that channels and bars can freely adapt their shapes to changes in the tidal and fluvial regime or to human impact (Hibma et al., 2004; Leuven et al., 2016, 2018b; Van Veen, 1950; Van Veen et al., 2005) (i.e. they are assumed to be fully alluviated [Leuven et al., 2018b; Savenije, 2015]). Tidal bar and meander dimensions are mainly determined by local estuary width in accordance with physical bar theories (Leuven et al., 2016). Nevertheless, from geological case studies it is well-known that geological constraints not only determine the initial position of the estuary from which the modern estuary evolved (De Haas et al., 2018; Townend, 2012), but can also form obstacles causing flow deflection in estuaries (Burningham, 2008; Heap & Nichol, 1997) and determine tidal inlet geometry (Bertin et al., 2004; Fitzgerald et al., 2000). Local effects by resistant self-formed clay layers on channel erosion also have been reported in tidal environments (Brückner et al., 2020; Fagherazzi & Furbish, 2001; Gruijters et al., 2004; Van de Lageweg et al., 2018; Ralston & Geyer, 2009; Schaumann et al., 2021). They may lead to hampering of channel incision or lateral migration (van der Wegen & Roelvink, 2012), limit the cross-sectional area of tidal inlets (Monbaliu et al., 2014) cause irregular local bottom topography, for example edges or scours (Hoitink et al., 2017; Huismans et al., 2016, 2021; Sloff et al., 2013), and are also suggested to locally affect channel and bar dimensions, positions and channel sinuosity (Dam et al., 2016; van der Wegen & Roelvink, 2012). Also in fluvial systems, resistant layers are known to limit channel erosion and influence channel pattern (Candel et al., 2020), as well as affect the morphology of the channel floor for example Mississippi (Nittrouer et al., 2011), Mekong (Allison et al., 2017) and Rhine-Meuse delta (Huismans et al., 2021). The effects of these constraints on the long-term evolution have hardly been assessed on the scale of an entire estuary. It therefore remains unknown to what degree channel-bar patterns in estuaries and the shape of estuaries are self-formed or controlled by initial conditions. This currently poses limits to realistic scenarios in state-of-the-art morphodynamic models that assume full alluviation (Van Der Wegen, 2013). By understanding and including the effects of resistant layers it will be possible to better predict changes in flood safety (Monbaliu et al., 2014; Van Wesenbeeck et al., 2014), navigability (Van Dijk et al., 2020; Wilson et al., 2017) and valuable habitat evolution (Chen et al., 2016; Kleinhans et al., 2021) in response to sea-level rise and other increasing human pressures.

Analysed here are the effects of resistant layers, and their varying degree of exposure over time at the channel base, on the shape and tidal bar pattern of the Ems-Dollard estuary, situated on the Dutch-German border (Figure 1). This estuary is a classic example of self-formed systems evolved in cohesionless sediments, ever since its channel-bar patterns with mutually evasive ebb and flood-dominated channels were described as typical for tidal environments by Van Veen (1950). However, its substrate is not only sandy, but erosion-resistant Pleistocene clays and tills occur at critical positions in the system. Two unique detailed datasets on historical bathymetry and subsurface composition are combined to track channel and node (i.e. confluence) locations, bar positions and bar dimensions through time and directly connect this to the presence of resistant layers. In this way, it is possible to demonstrate how such inherited resistant layers forced channel-bar morphology on a system-scale. Using published data of other systems, the effects of resistant layers are shown to be common worldwide.

2 | GEOLOGICAL AND GEOGRAPHICAL SETTING

In this section, the Pleistocene and Holocene substrate of the study area is described, which is summarised in Figure 2. In addition, Holocene estuary evolution and changing hydrodynamics are outlined. In the results section, the more detailed position of resistant layers and their effects on estuary evolution are shown.

20554877, 2023, 2, Downloaded from https://onlinelibrary.wiley.com/doi/10.1002/dep2.184 by Utrecht University Library, Wiley Online Library on [13/09/2023]. See the Terms and Conditions (https://onlinelibrary.wiley.com/terms-and-conditions) on Wiley Online Library for rules of use; OA articles are governed by the applicable Creative Commons License

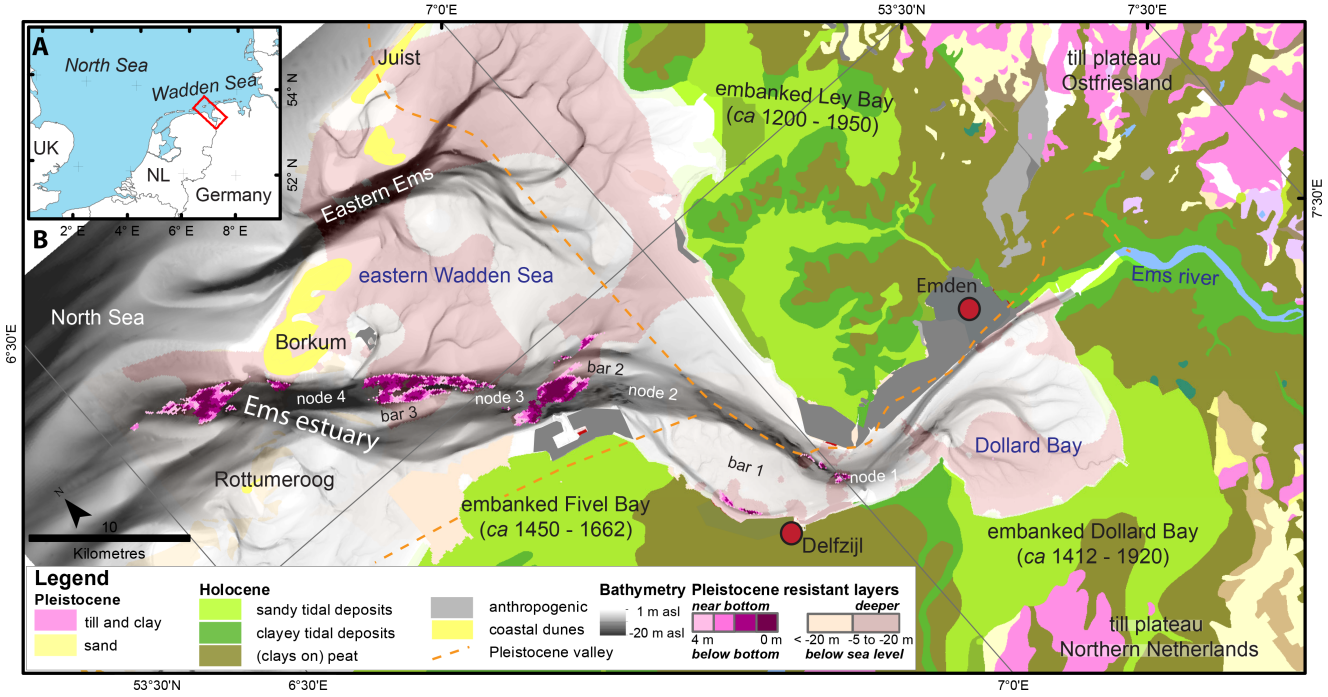

FIGURE 1 (A) Location of the study area. (B) Bathymetry of the Ems-Dollard estuary in 2005 with surrounding geology and the reconstructed position of resistant layers. Purple tones indicate where Pleistocene resistant layers (tills and clays combined) are close to the channel bottom (see Supplementary Materials section 1 for more detail on historical bathymetry). Resistant layers this study, see Figure 6. Geological map: Geologische Übersichtskarte 1:200,000 -https://produktcenter.bgr.de/terraCatalog/Start.do. Dashed lines: likely position of Late Pleistocene valleys after Hepp et al. (2019); TNO-GSN (2021a); course on land redrawn after map 'relief of the Holocene base' (NIBIS)

FIGURE 2 Schematic geological cross-section of the substrate of the estuary, used to design the workflow of compiling the layer models. Red dotted line indicates erosional contacts, black and grey lines represent the top of the Holocene and Pleistocene resistant layers respectively. Names correspond to the environmental interpretation in Table 1, all Pleistocene sandy deposits have been lumped into one unit in this illustration

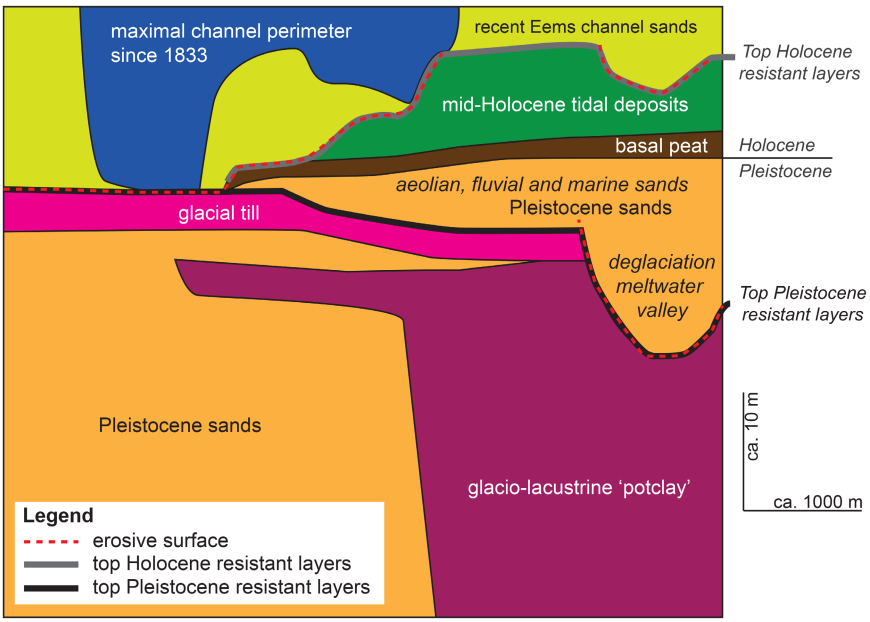

2.1 | Pleistocene substrate

The substrate of the Ems-Dollard estuary, within the depth reach of channels, mainly consists of Pleistocene and Holocene unconsolidated sands (Kruiver et al., 2017; TNO-GSN, 2021a), which are relatively easy to erode (Figure 2). This stratigraphy is interrupted by two strongly consolidated layers, interbedded within these erodible sands (Figure 2): Elsterian glacio-lacustrine clays (also known as 'potclays'; MIS 12 or 10; 475–420 or 370–330 ka BP) and glacial tills of Saalian age (MIS 6; *ca* 150 ka BP) (Peelo and Drente Formations respectively;

20554877, 2023, 2, Downloaded from https://onlinelibrary.wiley.com/doi/10.1002/dep2.184 by Utrecht University Library, Wiley Online Library on [13/09/2023]. See the Terms and Conditions (https://onlinelibrary.wiley.com/terms-and-conditions) on Wiley Online Library for rules of use; OA articles are governed by the applicable Creative Commons License

TABLE 1 Geological units in the substrate of the estuary, with lithostratigraphy of the Geological Survey of the Netherlands (TNO-GSN 2021b). Resistant layers in **bold**, see Figure 2 for their schematic stratigraphical position

Age	Lithostratigraphy	General description	Age and environmental interpretation	Resistance to erosion
Pleistocene (>11.7 ka)	Peelo Formation, undiff.	Fine sands	Elsterian (MIS 12 or 10) glacio-lacustrine	−
	Peelo Formation, Nieuwwolda Member (potclay)	**Very compact and erosion-resistant clay layer**	**Elsterian (MIS 12 or 10) glacio-lacustrine**	++
	Drente Formation, Gieten Member	**Very compact and erosion-resistant clay layer, containing abundant silts, sands and gravel**	**Saalian (MIS 6) glacial till**	++
	Drente Formation, Schaarsbergen Member	Sandy meltwater deposit, position in valleys cutting off older deposits	Saalian (MIS 6) deglaciation meltwater valley infill	−
	Eem Formation	Marine and tidal fine sands	Eemian (MIS 5e) marine and tidal deposits	sandy facies: − clayey facies: + mainly absent in study area
	Boxtel Formation	Sandy aeolian deposits (coversands), periglacial and (local) river sands.	Weichselian (MIS 5d−2) local aeolian and periglacial fluvial deposits	−
Holocene (<11.7 ka)	**Nieuwkoop Formation, Basal Peat Bed**	**Compacted erosion-resistant peat layer**	**Mid Holocene peat swamp**	+
	Nieuwkoop Formation, (excluding the Basal peat bed) + Naaldwijk Formation, Wormer Member	**Erosion-resistant clay and peat layers**	**Peat swamps, mid Holocene tidal deposits**	+
	Naaldwijk Formation, Walcheren Member	Mainly sands, locally mud	Late Holocene tidal deposits, recent Ems deposits	±

TNO-GSN, 2021a, 2021b). Both resistant layers crop out locally in the estuary and are present underneath the wider coastal plain, although locally they have been substantially eroded by glacial meltwater (Van den Berg & Beets, 1987). Elsterian glacio-lacustrine clays were deposited in a network of former glacial tunnel valleys of several kilometres wide and up to hundreds of metres in depth (Huuse & Lykke-Andersen, 2000; Praeg, 2003; TNO-GSN, 2021a). These clays became overconsolidated due to ice-loading during the late Saalian glaciation. This same ice sheet formed an up to *ca* 2 m thick till sheet that consists of a mixture of strongly consolidated clays, silts, sand and gravel (Rappol, 1987). Till ridges generally have a ENE-WSW orientation, reflecting former ice movement, and are flanked by meltwater valleys infilled with erodible sands (Van den Berg & Beets, 1987; Pierik, 2010). Eemian marine sands locally occur in the study area as well as Weichselian periglacial and aeolian sands (Eem and Boxtel Formations; TNO-GSN, 2021a; 2021b). The Late Weichselian course of the Ems (palaeo-Ems valley) was different from the current position of the Ems river and estuary (Figure 1). It followed a more northerly course near Emden (well-mapped by Barckhausen & Streif, 1978) and Barckhausen (1984), where the resistant Elsterian potclay is positioned relatively deep. Under the current estuary, its course is more uncertain, but it probably ran west, just south of the current estuary, where the base of the Pleistocene deposits are lower (TNO-GSN, 2021a). A northern branch possibly existed as well, 40 km north of the island of Juist. A palaeovalley was traced in seismics and linked to the Late Weichselian/Early Holocene Ems by Hepp et al. (2019). The current spatial configuration of both the tills and the glacio-lacustrine clays is the result of the position of these tunnel valleys, till ridges and the post-glacial erosion valleys.

2054877, 2023, 2, Downloaded from https://onlinelibrary.wiley.com/doi/10.1002/dep2.184 by Utrecht University Library, Wiley Online Library on [13/09/2023]. See the Terms and Conditions (https://onlinelibrary.wiley.com/terms-and-conditions) on Wiley Online Library for rules of use; OA articles are governed by the applicable Creative Commons License

2.2 | Holocene substrate and evolution

The Holocene coastal wedge on top of the resistant layers consists of a succession of sand, clay and freshwater peat (Figure 2). Its thickness ranges from 15–25 m close to the coastline to 5–8 m inland (Kruiver et al., 2017; Roeleveld, 1974; Streif, 2004; TNO-GSN, 2021a). The coastal wedge is thickest and oldest where Late Pleistocene inherited valleys were present in the landscape. Especially the locally preserved layers at the base of the Holocene wedge, compacted early Holocene basal peat (Nieuwkoop Formation; Basal Peat Bed; TNO-GSN, 2021b) and mid Holocene tidal clays (Vos & Van Kesteren, 2000; Naaldwijk Formation, Wormer Member; TNO-GSN, 2021b), form moderately resistant layers. The mid Holocene tidal deposits are generally sandy around former channels and more clayey toward the edges of the basin with occasional peat intercalations (Barckhausen & Streif, 1978; De Haas et al., 2018; Roeleveld, 1974; Vos & Van Kesteren, 2000). They formed before 4000 yr BP and are positioned below −5 m Mean Sea Level (MSL) (Hijma, 2016). In the second half of the Holocene, the Ems was a river with modest tidal influence, positioned in a coastal peatland environment, debouching into the Wadden Sea (Behre, 1999, 2004; Vos & Knol, 2015). These peatlands were reclaimed from the Middle Ages onwards, the Ems was embanked from around the year AD 1000 to the 13th century (Ey, 2010; Oost, 1995; Vos & Knol, 2015). The peatland drainage resulted in land subsidence (Vos & Knol, 2015), but marine influence along the river was still relatively small. This changed, however, as major land losses occurred in the 13-16th centuries forming the Dollard Bay (50 km inland) (Stratingh & Venema, 1855). This happened after a series of storm surges into reclaimed and subsided peatlands with too weak embankments (Pierik et al., 2017; Vos & Bungenstock, 2013; Vos & Knol, 2015). Former peatlands were eroded and the effects of tides became significantly larger. The tidal prism of the estuary increased significantly (by *ca* 350 km^2), enlarging the major channels (Van Maren et al., 2016). In the centuries afterwards, Dollard Bay was gradually infilled, forming supratidal flats that were successively embanked (Esselink et al., 2011; Homeier, 1962, 1977; De Smet, 1962). The Ems channel, bar and tidal flat deposits formed over the last centuries are generally sandier than the mid Holocene tidal deposits because they formed under higher energy conditions. In the 20th century, human impact on the estuary increased further. Deepening of the upstream tidal river, substantial dredging and the creation of large harbours changed tidal and sediment dynamics in the system (Van Maren et al., 2016). Also, tidal discharges, volumes and current velocities have increased between 1937 and 2005 (Herrling & Niemeyer, 2008). The tidal range at the entrance of the estuary, is currently around 2 m (Borkum), which has not significantly changed over the past several thousand years. In the current estuary, tidal range near the cities of Emden and Delfzijl is around 3 m. The Ems river has a mean annual discharge of 81 m^3 s^{-1}.

3 | MATERIALS AND METHODS

To study the effect of resistant layers on the channel pattern for the Ems-Dollard estuary in detail, historical bathymetry was mapped over the last two centuries and the position of the resistant layers was reconstructed in high spatial resolution. To do so, new cross-sections were compiled and a new geological GIS dataset was collected showing the occurrence and depth of resistant layers. Finally, to determine effects of geology on historical evolution, channel dimensions were quantified from the bathymetric time series along the estuary.

3.1 | Reconstruction and analysis of historical bathymetry

Bathymetrical changes throughout the last two centuries were used to trace potential effects of resistant layers over time. Bathymetry was extracted using historical maps of the Ems-Dollard estuary, compiled by the department of defence for 1833, 1888, 1928 and 1953. These maps were digitised and subsequently interpolated to 100 × 100 m grids. From 1985 onward detailed bathymetries are available (SI 1). Measurements for estuarine dimensions, that is width-to-depth (W/h) ratio and cross-sectional area (CSA) were extracted on cross-sections with a 200 m spacing along the estuary centreline, following (Leuven et al., 2018c). Bar length and spacing between the confluences (i.e. nodes) were measured along the centreline and compared to the local estuary width, which is defined as the channel width including bars.

3.2 | Layer modelling

The occurrence and position of resistant layers was reconstructed by compiling a geological layer model (Figure 3) using geological borehole data from the Dutch DINOLoket (https://www.dinoloket.nl/en; TNO-GSN, 2021b) and the German LBEG (https://nibis.lbeg.de/cardomap3/) data repositories. Boreholes with resistant layers were identified (Figure 4), and the top of these layers was interpolated into raster files that show the position of the

20554877, 2023, 2, Downloaded from https://onlinelibrary.wiley.com/doi/10.1002/dep2.184 by Utrecht University Library, Wiley Online Library on [13/09/2023]. See the Terms and Conditions (https://onlinelibrary.wiley.com/terms-and-conditions) on Wiley Online Library for rules of use; OA articles are governed by the applicable Creative Commons License

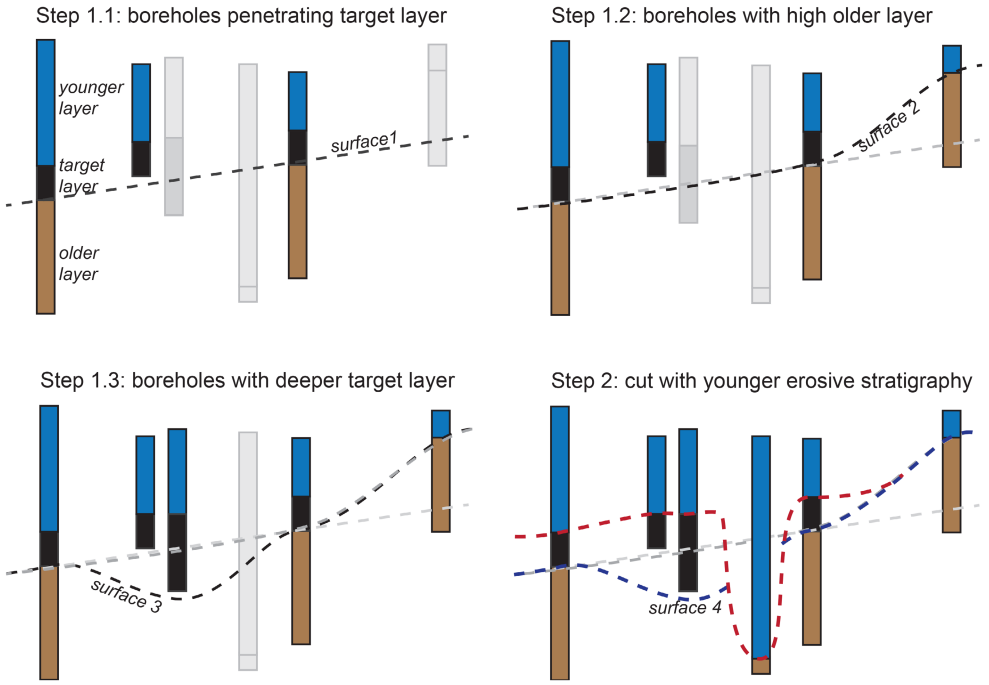

FIGURE 3 Iterative workflow for interpolating the base of resistant layers. In the first step, boreholes are selected that reach the resistant layers' bases, these serve as input for interpolation plane 'surface 1', In steps 1.2 and 1.3, this plane is adapted to boreholes in which the target layer is deeper or shallower. In step 2 all younger layers and bathymetry over all time steps are used to cut the plane. For the cases only the top of the target layer was reached whereas the base was not, the average thickness was subtracted from its top

resistant layers, following the procedure of Gunnink et al. (2013). To account for post-depositional erosion, younger erosive channel fills (e.g. glacial meltwater deposits, tidal channels) were identified from the borehole data and used to cross-cut the resistant layer raster files, following the conceptual stratigraphy in Figure 2.

Model steps are explained below and in Figure 3. Steps 1.1–1.3 were done for all target layers, that is the resistant layers and (lumped) other deposits that relate to them (in Table 1 and Figure 2). Step 2 was only performed for the resistant layers.

Step 1.1 - Selection of all stratigraphic bases of the target layer in the boreholes in which the base of the target layer was reached. These values were interpolated, resulting in surface 1 as a first approximation of the layers' base.

Step 1.2 - Selection of stratigraphic boreholes with tops that are older than the target layer but occur higher than surface 1. At these locations, the target layer is absent but higher, older topography is present. These points from steps 1.1 and 1.2 were interpolated, creating surface 2 as a second iterative step of the base of the target layer.

Step 1.3 - Selection of boreholes in which the target layer was reached, but its base was not. For these cases a theoretical base of 1 m below the end-depth of the borehole was defined, thereby forcing the to-be-interpolated surface below the depth of surface 2. A *topogrid* interpolation of surface 3 of the base of the target layer was applied using points from steps 1.1, 1.2 and 1.3.

Step 2 - After modelling the stratigraphic base of each layer, a stacked layer model was constructed with consistent stratigraphical cross-cut relationships (see Figure 2). For example, deposits associated with channels (e.g. the base of the deglaciation meltwater channel, Figure 3) dissect older deposits (e.g. tills and older Pleistocene sands), where they occur at greater depth. Because the LEBG borehole data were labelled manually, the workflow had to be adapted for these data: where resistant layers do not occur based on step 1.1, although expected, a channel structure was assumed that cuts them. The youngest Holocene Ems channel sands were labelled and used to cut all layers (no older layers could be present higher than this surface). The same was performed using bathymetry over the last 200 years, that is maximal depth over the last two centuries.

Step 2 results in a set of grids or layers of the base of each unit. Using these data, the top of any layer, including those of the resistant layers could be calculated and or combined. This was done by combining the maximal depth of the base of all younger deposits.

20554877, 2023, 2, Downloaded from https://onlinelibrary.wiley.com/doi/10.1002/dep2.184 by Utrecht University Library, Wiley Online Library on [13/09/2023]. See the Terms and Conditions (https://onlinelibrary.wiley.com/terms-and-conditions) on Wiley Online Library for rules of use; OA articles are governed by the applicable Creative Commons License

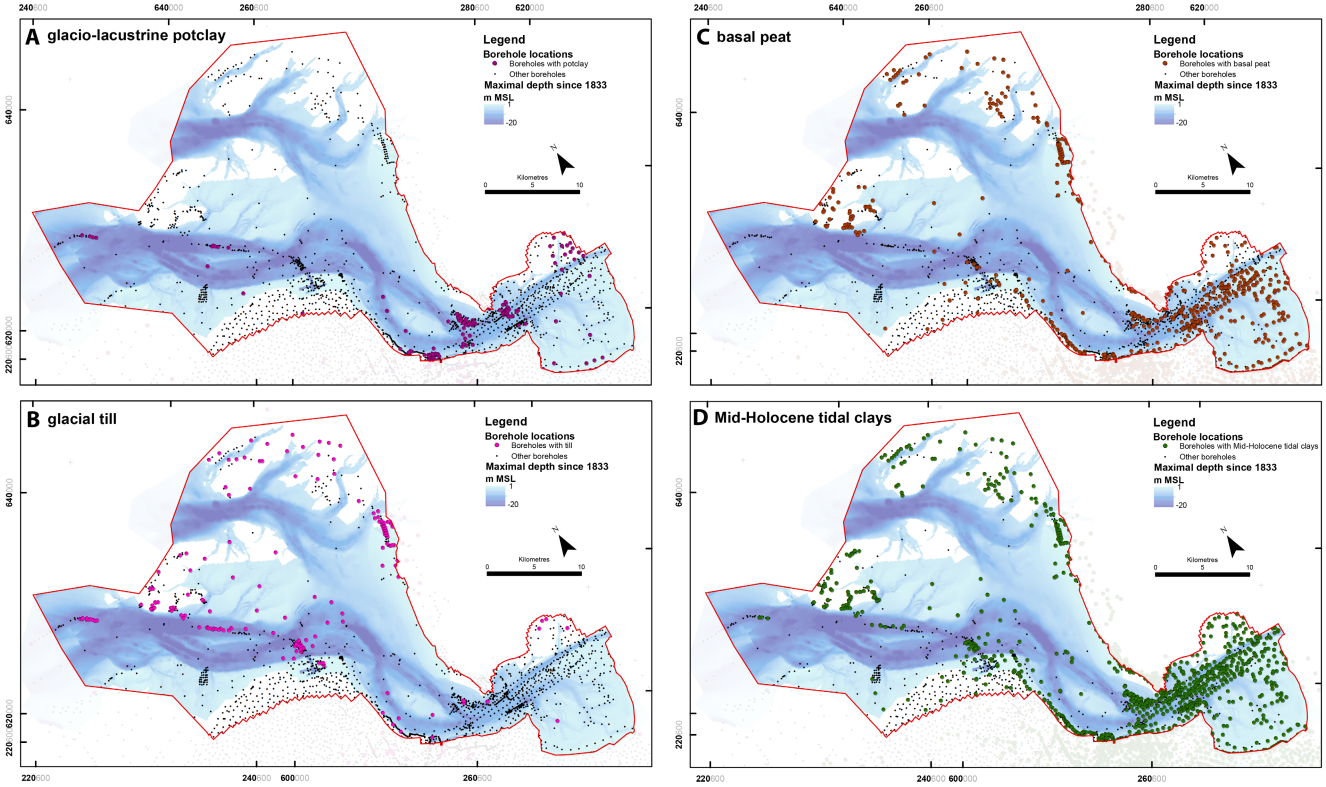

FIGURE 4 Boreholes in the Ems-Dollard estuary used for grid interpolation for all Pleistocene and Holocene resistant layers separately. Coloured boreholes indicate where resistant layers were encountered. Deepest position of estuary channels since 1833 indicated in blue (i.e. deepest points of all bathymetry datasets combined). Borehole data from the Geological Surveys of the Netherlands and Lower Saxony. Projection in Dutch coordinate system RD New (EPSG: 28992)

4 | RESULTS

4.1 | Position of resistant layers in new geological reconstructions

In this section the existing geological insights of the study area are supplemented with new and more detailed information on the position of Pleistocene resistant and Holocene resistant layers. For this the detailed cross-sections and new raster layer files are used (Figures 5 and 6). Where relevant, other (less resistant) units were considered as well, for example in the cases where these may represent infillings of old deglaciation meltwater valleys that dissected older Pleistocene resistant layers (see Figure 2).

The new raster layer files and cross-sections show that the erosion-resistant layers are present in the estuary's substrate at several distinct locations (Figures 5 and 6). The glacio-lacustrine potclay is close to or at the channel floor on three locations: in the northern channel around bar 3 at −18 m MSL, along the western channel of bar 1 at −15 m, and around node 1 around 15 m (Figures 5, 6A and 7). Tills are present in the northern channel around bar 3 on top of the potclay (Figure 5: E–E' and F–F'). Near bar 2, a ENE-WSW oriented till ridge was found around 13 m depth (Figure 5: F–F'; 4B and 6). This orientation is in line with till ridges on either side of the estuary on land (Van den Berg & Beets, 1987; Pierik, 2010; Figure 1). These deposits are generally covered by Weichselian coversands and periglacial fluvial deposits, reaching several metres thick. This cover is generally absent where Holocene erosion occurred (Figure 5).

As in the adjacent till plateaus, small and large meltwater valleys have locally eroded these layers before the Holocene. Where the Holocene estuary crosses these sandy infilled Saalian meltwater valleys, deeper tidal erosion was facilitated, and the confluences preferentially formed (nodes 2,3,4 in Figure 6A). The presence of coarser fractions in the bed (D50 >300 μm Oberrecht et al., 2016: their Figure 8) show that the till has been eroded by abrasion to some degree. These resistant layers have, however, been persistently visible in the bathymetry over the last 200 years, which confirms their high resistance to tidal channel erosion.

In the study, several generations of Late Pleistocene (Ems) valleys are present with different orientations, two of which could be mapped. A Late Weichselian/Early Holocene Ems palaeovalley was convincingly

20554877, 2023, 2, Downloaded from https://onlinelibrary.wiley.com/doi/10.1002/dep2.184 by Utrecht University Library, Wiley Online Library on [13/09/2023]. See the Terms and Conditions (https://onlinelibrary.wiley.com/terms-and-conditions) on Wiley Online Library for rules of use; OA articles are governed by the applicable Creative Commons License

demonstrated north of Emden (Barckhausen, 1984; Figure 5: A–A'). A second, relatively large meltwater channel (ESE-WNW) was found running south of the most downstream part of the estuary. It is filled with sandy glaciofluvial sediments and topped by Weichselian aeolian coversands (Figure 5: E-E' and 6). The base of the Holocene is located relatively low along its course (Figures 5 and 6; TNO-GSN, 2021a). This valley probably formed during the Saalian deglaciation and may have been active during the Eemian and a substantial part of the Weichselian as well. In addition, a northern branch may be present, connecting to the presumed Ems palaeovalley north of Juist (Hepp et al., 2019). In the study area, its most likely course would be through *cross-section D–D'* (Figure 5) (base pre-Holocene around −20 m), around the current position of the *Oostfriesegaatje*. The till ridge (around bar 2 in Figures 1 and 6A) with its top around −13 m MSL (Figure 5: F–F'), must have been a barrier in the landscape, so probably the valley ran just east of it, through an area with very low data density (Figure 4A,B).

The cross-sections and raster layer files also show that Holocene tidal clays and peat are found at the channel margins and also at the channel base in the most landward part of the estuary (Figures 4C,D and 5). Where the top of the

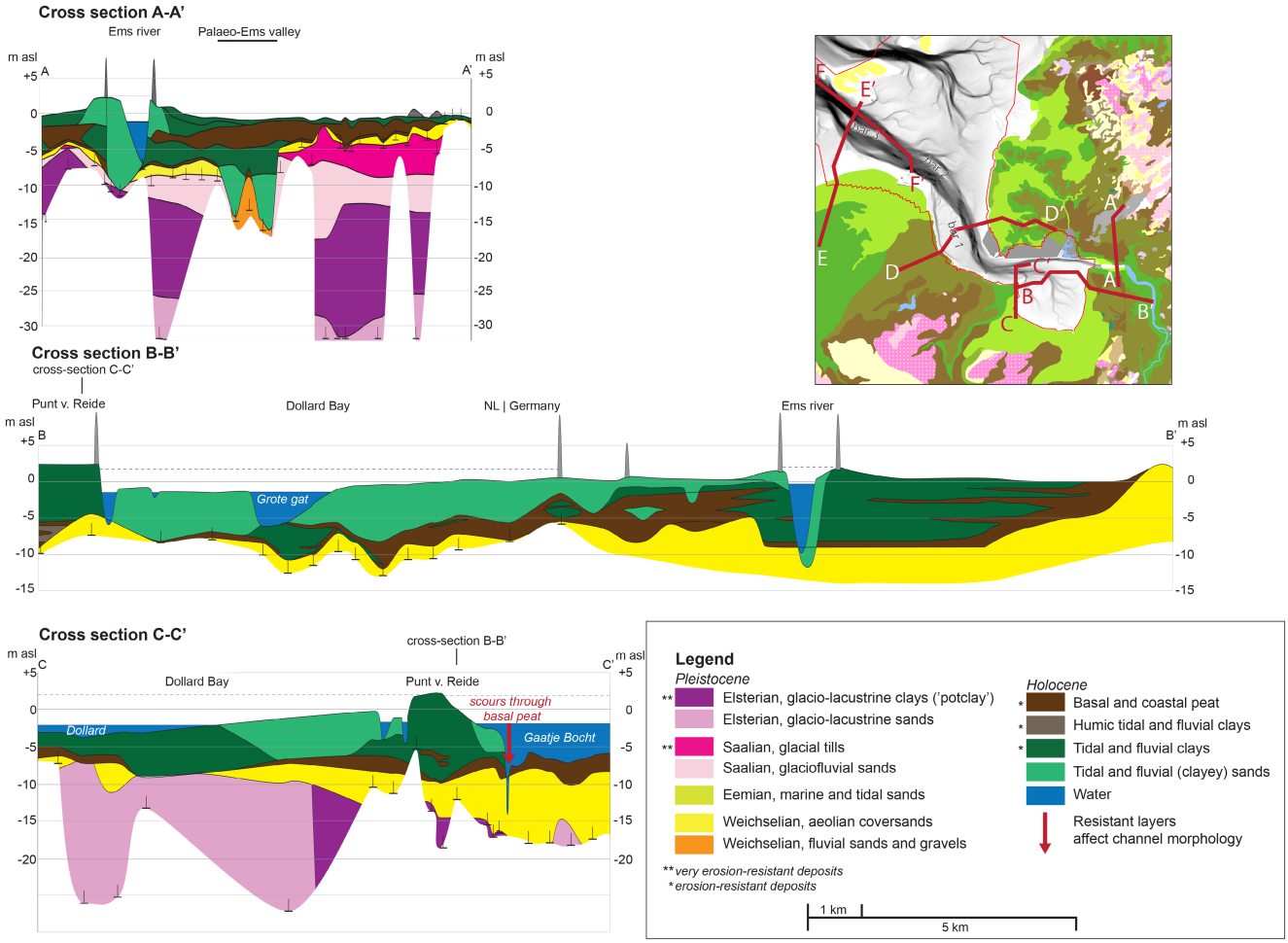

FIGURE 5 Geological cross-sections in and around the Ems-Dollard estuary. Geological units in the map inset same as in Figure 1. Borehole data derived from borehole databases of the Geological Surveys of the Netherlands and Lower Saxony, supplemented with existing cross-sections. Channel bathymetry is from 2014. A–A': cross-section after Barckhausen (1984) showing the Late Weichselian/Early Holocene palaeo-Ems valley north of the current Ems following a zone where resistant glaciofluvial clays are positioned lower. B–B': German part in after Streif (2004). Dollard Bay infill on top of peat and the Ems river embedded in Holocene peat and clays can be seen. C–C': Holocene peat at the channel base with scours up to *ca* −15 m below sea level (see also bathymetry in Figure 9C). D–D': part west from *Bocht van Watum* after Roeleveld (1974), part east of Ems after Barckhausen and Streif (1978). Palaeo-Ems valley likely positioned under the current main estuary channel, clay and peat on its flanks cause edge effects in bathymetry (Figure 9B). E–E': Geology in northern Ems channel (*Ranzelgat*) after Jonkman and De Vries (2010). Pleistocene clays hamper channel deepening, south of the estuary a large Late Pleistocene meltwater valley is likely present, formed by Saalian meltwater and likely also active in the Weichselian (Figure 6). F–F': Cross-section through dredged shipping channel after Jonkman and De Vries (2010) showing presence and absence of Pleistocene clays on the channel bottom

20554877, 2023, 2, Downloaded from https://onlinelibrary.wiley.com/doi/10.1002/dep2.184 by Utrecht University Library, Wiley Online Library on [13/09/2023]. See the Terms and Conditions (https://onlinelibrary.wiley.com/terms-and-conditions) on Wiley Online Library for rules of use; OA articles are governed by the applicable Creative Commons License

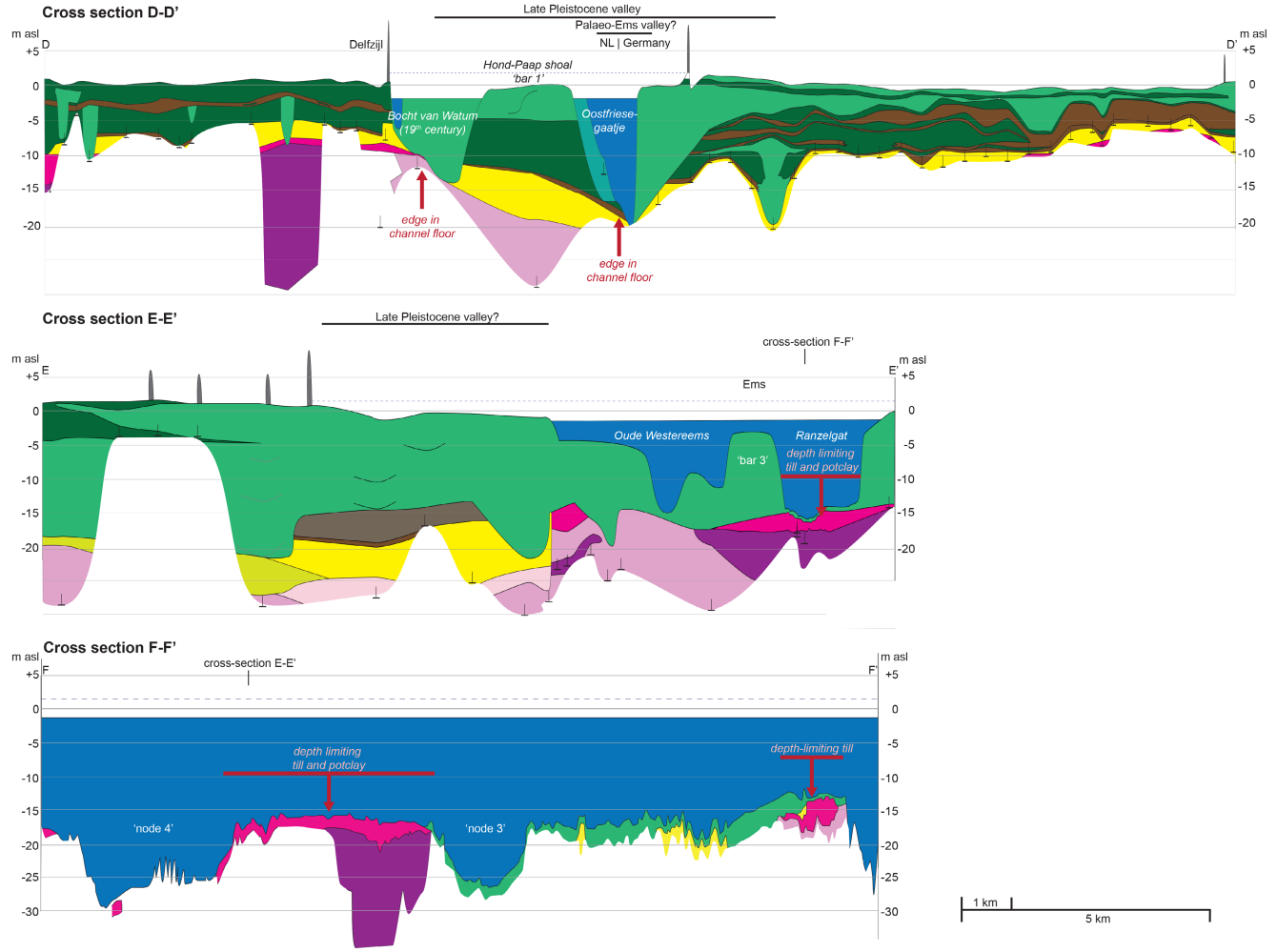

FIGURE 5 (Continued)

Pleistocene surface is deeper (e.g. at the position of old dissecting valleys), these layers are also generally positioned deeper (e.g. in Figure 5: D–D'). Especially these deeper peat and clays are most compressed under the weight of several metres of sediments making them relatively resistant to erosion. Towards the sea, the Holocene tidal deposits are more sandy, reflecting an increasing energy gradient towards the mouth of the estuary. Perpendicular to the estuary, Holocene sediments become finer as well and the flanking peatlands contain layers of tidal clays (Figure 5: D–D'), representing distal coastal swamp environments with a varying degree of marine influence.

4.2 | Reconstructed bathymetry and changes in channel volume

The bathymetry dataset starts in the 19th century and shows relatively large channels in which resistant layers are well-exposed (e.g. till ridge in segment 2; Figures 1, 5 and 7). Since the 19th century, the channels have shown a net import of sediment, of 1–3 Mm^3 per year, burying most resistant layers at the channel base. Most likely the system adapted to the stepwise decreasing tidal prism by embankment of the Dollard in the preceding centuries (Van Maren et al., 2016) (Figure 7). In the most seaward section (segment 1) a contrasting trend is observed in the 19th century. Here, channel volume became larger instead of smaller by *ca* 1.4 Mm^3/yr, probably as a reaction to the silting up of the Eastern Ems (Figure 1).

From the beginning of the 19th century to the 1960s, the system had four nodes and two channels with a relatively large meander curvature (Figure 7C,D,E). This changed as the *Oostfriesegaatje* (eastern channel around bar 1 in segment 3) became larger after AD 1900, while the *Bocht van Watum* (western channel around bar 1) became smaller (Gerritsen, 1952; Van Maren et al., 2016; Figure 7D,E,F 'marked I'). These developments decreased channel sinuosity around bars 2 and 3 from 1.28–1.31 in 1833 to 1.08–1.01 in 1928 (Figure 8B).

20554877, 2023, 2, Downloaded from https://onlinelibrary.wiley.com/doi/10.1002/dep2.184 by Utrecht University Library, Wiley Online Library on [13/09/2023]. See the Terms and Conditions (https://onlinelibrary.wiley.com/terms-and-conditions) on Wiley Online Library for rules of use; OA articles are governed by the applicable Creative Commons License

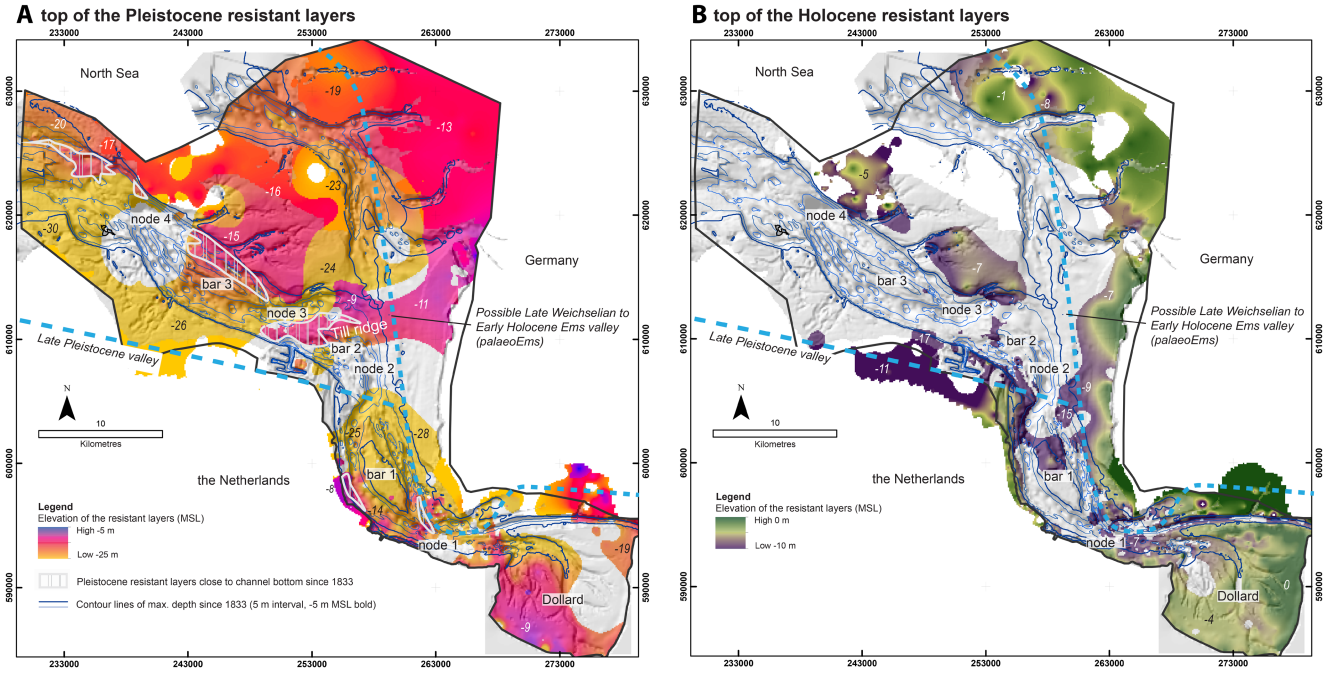

FIGURE 6 Grid interpolations of (A) the Pleistocene layers: glacio-lacustrine clays and glacial tills combined and (B) Holocene layers: peat and tidal clay combined. Workflow in Figure 3, source data in Figure 4. Most likely routes of the Late Pleistocene valleys are indicated, they generally coincide with deeper or absent Pleistocene resistant layers. Position of bars is coeval with shallow occurrence of resistant layers; nodes preferentially form where resistant layers are absent or deep. Hillshade and contour lines are shown for the maximum channel depth since 1833 (i.e. the deepest position of all bathymetry sets combined). Projection in Dutch coordinate system RD New (EPSG: 28992)

Over the last 50 years human impact increased significantly through land reclamation, new harbours and dredging (Van Maren et al., 2015). Between 1953 and 1985 the total channel volume increased by *ca* 200 Mm^3 (0.3 Mm^3/yr in segment 4 to 2.7 Mm^3/yr in segment 1 – Figure 7A), which equals an average of 1 m for the entire estuary. This is in accordance with the 134 Mm^3 that has been extracted between AD 1960 and 1985 (Mulder, 2013; Figure 7B).

4.3 | Effects of Pleistocene resistant layers

Discussed here are the effects of resistant layers on the dimensions and position of channels and bars. In the discussion section, their local and regional impact are compared and the wider implications are shown. At locations where erosion-resistant Pleistocene clays and tills outcrop (*ca* 10–15 m below MSL: Figure 8A), channels are less deep and the estuary is relatively wide. These trends are most prominent around bars 2 and 3 and on the bathymetry of the 19th century, when channel volume was relatively large (Figure 7). At places where the Pleistocene resistant layers are present at or close to the channel floor, channel width-to-depth ratios vary between 400 and 800 with a quasi-periodic pattern in longitudinal direction, reflecting the outcrop positions (Figure 8D). Meanwhile, the cross-sectional area (CSA) of the channels decreases approximately linearly in landward direction for all time steps (Figure 8C). This implies that, to maintain this linear longitudinal trend in CSA (Figure 8C,D), the channels have increased their widths where the equilibrium depth was limited by resistant layers. Where present, the resistant layers caused lateral channel migration and outer bank erosion, rather than channel deepening. This resulted in curved channels around non-migratory mid-channel bars (Leuven et al., 2018b), present between 6–12, 20–25, 27.5–36 km (orange shadings in Figure 8C,D). Subsequent estuary widening allowed the width of bars to increase. This mechanism explains the preferential occurrence of mid-channel bars where resistant layers are present (Figure 8A). These allogenically forced bars alternate with relatively deep and narrow channel confluences (nodes). These occur where the resistant layers are absent or too deep, for example because these zones are positioned in former Saalian meltwater valleys, filled in with Pleistocene erodible sands, flanking the till ridges (Figures 6A and 8A around 15–25 km, the latter only before 1928).

20554877, 2023, 2, Downloaded from https://onlinelibrary.wiley.com/doi/10.1002/dep2.184 by Utrecht University Library, Wiley Online Library on [13/09/2023]. See the Terms and Conditions (https://onlinelibrary.wiley.com/terms-and-conditions) on Wiley Online Library for rules of use; OA articles are governed by the applicable Creative Commons License

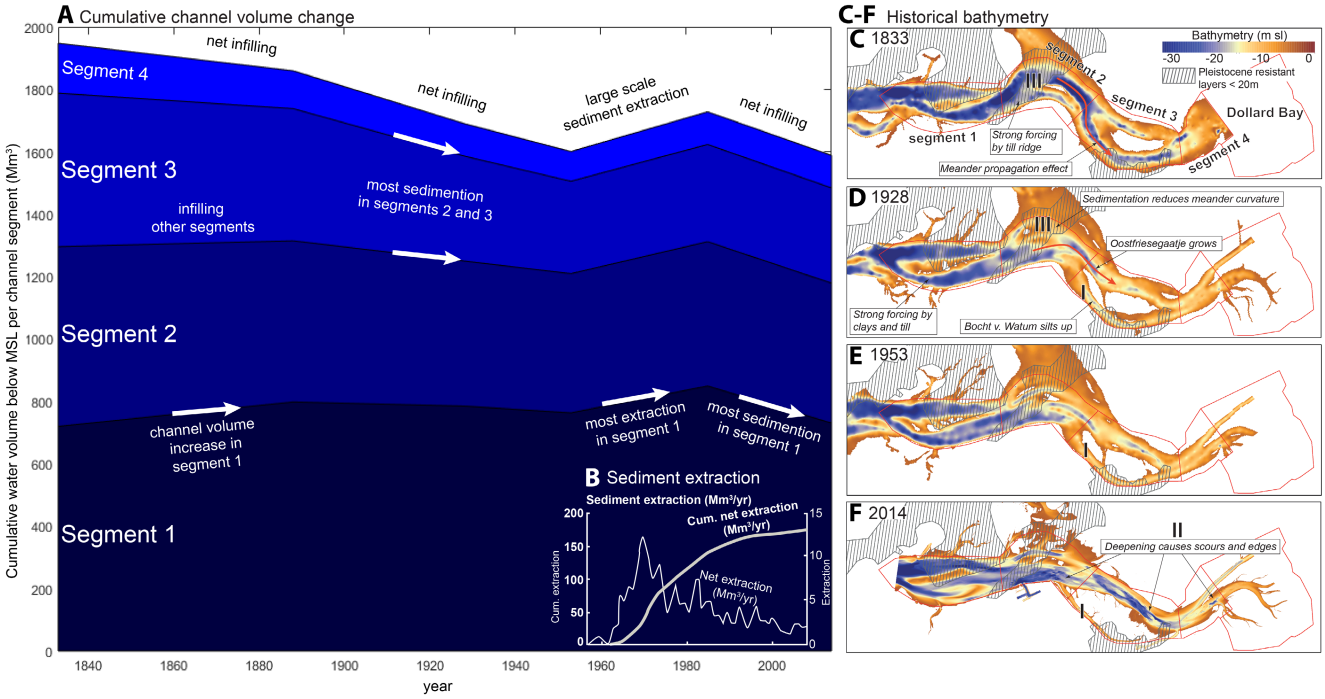

FIGURE 7 (A) Volume changes of the channels (water volume relative to current MSL) since 1833 per segment. Segments are numbered from the coastline landinward (C). (B) The total net extraction in the inset includes sand mining and dredging volumes (that were not dispersed again) (Mulder, 2013). In total, *ca* 140 Mm^3 has been extracted from the system between 1953 and 1985, which corresponds to the channel volume increase found for this period in this study. (C–F) Bathymetry and channel volume reduction per segment for the subtidal areas between 1833 and 2014, based on depth measurements in historical maps. Hatching indicates presence of resistant tills and glaciofluvial clays above −20 m MSL (see Figure 6A). Bathymetrical data of the Dollard bay are not available for 1833 and 1953. Position of the resistant layers around moderate channel depth coincide with the presence of wide meander bends and a large total width of the estuary

4.4 | Effects of Holocene resistant layers

Where Holocene peat and clays form the bottom of the channel floor, channel deepening is hampered as well. Their thickness and their degree of erosion resistance are, however, smaller compared to the Pleistocene clays and tills, and therefore scour holes and edges formed more easily (Figure 5: C–C'; Figure 9A,C). These features formed at places where the channel has become deeper over the last century (e.g. *Oostfriesegaatje*, *Gaatje Bocht* Figures 7E,F and 9). These scours penetrate layers of clay and peat and then encounter Pleistocene sands that they can more easily erode, making them relatively deep, as described by Huismans et al. (2016, 2021) for scours in the Rhine-Meuse delta. Sharp edges are observed (Figure 9B) over longer distances in the channel east of bar 1 in segment 3. This channel (*Oostfriesegaatje*) has deepened over the last two centuries, exposing these older layers that were probably formed in early stages of Holocene transgression along the palaeo-Ems valley (Figures 1 and 5: D–D'). In the southern part of Figure 9B (*Gaatje Bocht*), the very base of the scour is limited by the occurrence of Pleistocene clay.

5 | DISCUSSION

5.1 | Resistant layers: a local or an estuary-wide effect?

The position of nodes and bars in the Ems-Dollard estuary are thus forced by the distribution pattern of resistant layers to a large extent, rather than resulting from changing hydrodynamic boundary conditions. Depth-limiting resistant layers result in channel widening, local bank erosion, and mid-channel bar formation, while deeper nodes preferentially occur where resistant layers are absent. This means that erosion-resistant layers at depth can have similar effects on bar and bend morphology as horizontal topographic forcing, for example by erosion-resistant banks, has long been known to have (van Dijk et al., 2012; Leuven et al., 2018c). These effects directly force at least two *ca* 10 km long bars (bars 2 and 3), over half the length of the estuary. These effects do not only occur locally at the positions of resistant layers; forced channel curvature around bar 2 (S = 1.28 in 1833; Figure 8) propagates to the next meander bend, favouring the branch connected to the outer bend at the bifurcation in the *Bocht van Watum* (during ebb flow)

20554877, 2023, 2, Downloaded from https://onlinelibrary.wiley.com/doi/10.1002/dep2.184 by Utrecht University Library, Wiley Online Library on [13/09/2023]. See the Terms and Conditions (https://onlinelibrary.wiley.com/terms-and-conditions) on Wiley Online Library for rules of use; OA articles are governed by the applicable Creative Commons License

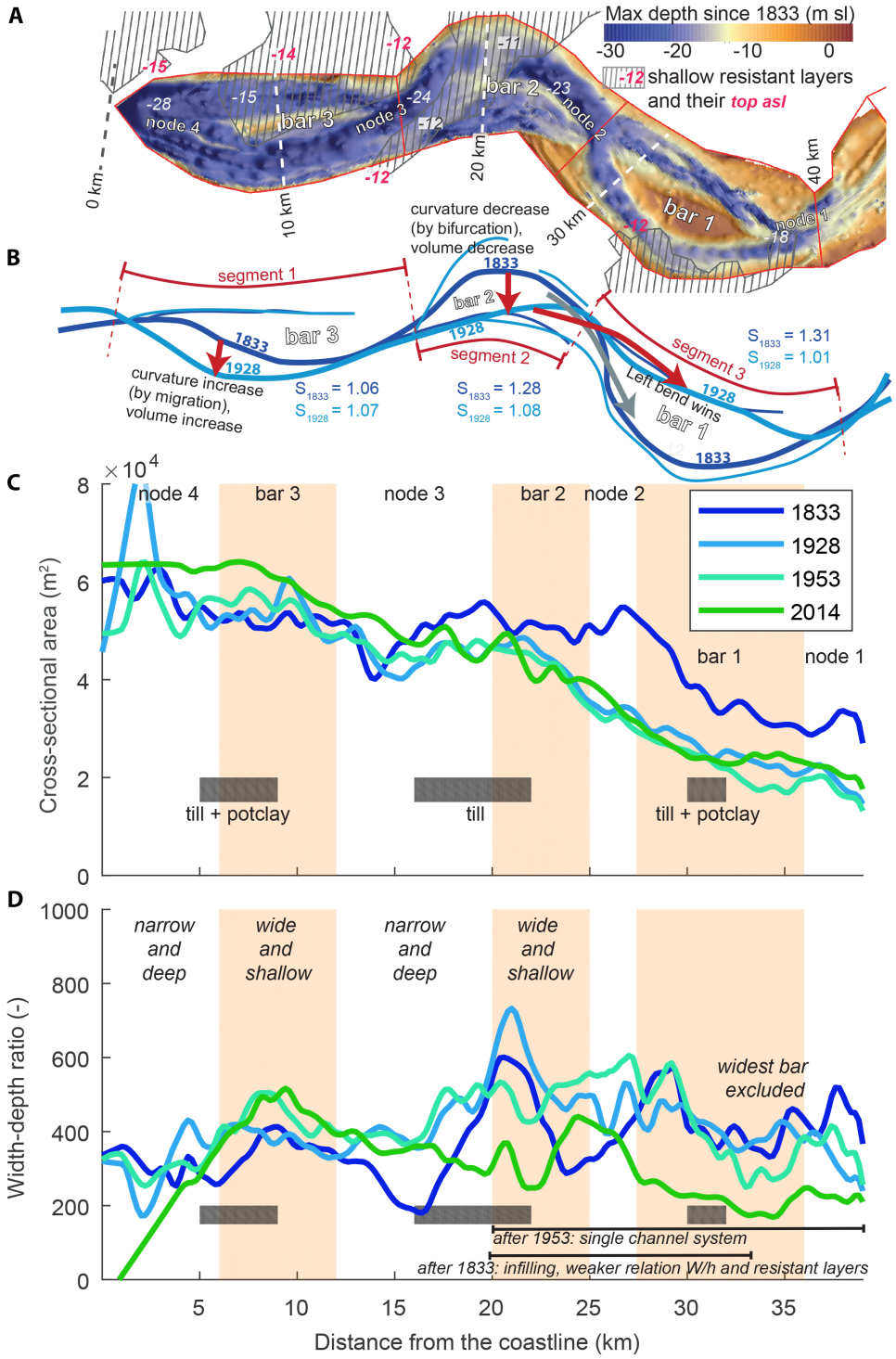

FIGURE 8 Effect of Pleistocene resistant layers. (A) Maximum depth since 1833 shows that shallow and wide parts of channels have been persistently present where resistant layers occur and confluences (nodes) occur where they are absent. Bar positions were relatively persistent over time. (B) Centrelines for 1833 and 1928 indicate meander migration in segment 1 in response to volume increase (Figure 7). The opposite is seen in segments 2 and 3. Here, channel volume decrease making the straight bifurcates most suitable. Sinuosity (S) is shown per segment. (C) Channel cross-sectional area (CSA) in m^2 along the estuary shows a roughly linear decrease in landward direction, independent of occurring bar pattern and geology. Intervals with depth-limiting resistant layers indicated in grey blocks. (D) Width-to-depth (W/h) ratio along the estuary. High W/h ratios occur where resistant layers are present and when exposed on the channel bed. Nodes 3 and 4 have been most persistent over time, likewise the W/h ratio trends remained relatively constant. Node 2 rapidly shallowed after the 19th century, yielding more diffuse trends in W/h ratio over time. The shallowest and flattest subtidal area values (above −3 m MSL roughly above the lowest spring tide) were excluded to focus on evolution of the channels. Because bar 1 is above that, an apparent dip in W/h occurs here. The landward reach reduced in CSA over time (C), mainly due to narrowing (D)

20554877, 2023, 2, Downloaded from https://onlinelibrary.wiley.com/doi/10.1002/dep2.184 by Utrecht University Library, Wiley Online Library on [13/09/2023]. See the Terms and Conditions (https://onlinelibrary.wiley.com/terms-and-conditions) on Wiley Online Library for rules of use; OA articles are governed by the applicable Creative Commons License

(S = 1.31 in 1833; red arrow in Figure 7C). Similar effects of propagating meander curvature to the neighbouring bends have been observed in fluvial environments (Van Dijk et al., 2012). This cascade of meander and tidal bifurcation effects through the system means that the effects of resistant layers can also be expanded beyond local effects over at least one bar or meander wavelength.

If these resistant layers are so important, would the bar lengths and node spacing have been so different without their forcing effects? Global datasets show that alluvial bar lengths and node spacing scale with estuary width (Leuven et al., 2016, 2018b). For the Ems-Dollard these variables, especially bar 1 and 3 and their bounding nodes, plot on the upper range of those found in many modern tidal systems and in laboratory scale experiments. This applies especially to node spacing that lies outside or just within the 95% confidence range of other estuaries (Figure 10A,B). Bar lengths are relatively long, but still fall within the 95% confidence range. These patterns are attributed to the fact that the spacing of the resistant layers coincidentally falls within the hydromorphologically suited range for bar and node dimensions (i.e. the confidence interval in Figure 10). The Pleistocene resistant layers hence force the exact location and the actual dimensions within or very close to that confidence range.

There were no indications that the Holocene resistant peat and clays affected channel and bar patterns on the scale of the entire estuary. Most likely this was because they are not as resistant and thick compared to the Pleistocene clays and tills that affect the system on longer timescales. The Holocene resistant layers do, however, cause significant scours and edges, which may locally lead to unstable channel banks in case scour holes may grow towards them (Huismans et al., 2021).

5.2 | Human impact on exposure of resistant layers

Within the Ems-Dollard estuary an increase in channel volume can be seen that can be linked to a stronger forcing effect, while a decrease in channel volume (i.e. increased alluviation) correlates to less forcing by resistant layers. A good example of the former can be seen in the most seaward segment (segment 1), where channel volume has increased over the last century (Figure 7) and resistant Pleistocene layers became more exposed (Figure 5E–E' and F–F'), correlating with increased meander curvature and a higher W/h ratio (around 5 km) for the more recent timesteps (Figures 7D and 8B,D). In the more upstream segments, a similar correlation is observed. The diagonally oriented till ridge in segment 2 had forced the channel curvature to be high towards the beginning of the 19th century (outer bend bar 2 around ridge marked 'III' in Figure 7C). This probably happened because an increase in tidal prism, caused by the formation of Dollard Bay in the 16th century upstream (Van Maren et al., 2016), facilitated the formation of deeper channels between the 16th and 19th century, exposing this till ridge at their bases. As sedimentation continued over the last two centuries, this exposed till ridge was partly buried and meander curvature decreased (Figure 7D, sinuosity in segment 2 decreased from 1.28 in 1833 to 1.08 in 1928; Figure 8B). The tidal flow subsequentely preferred the *Oostfriesegaatje* over the *Bocht van Watum* since 1888 (Figure 7D). The latter eventually closed, straightening the channels in segments 2 and 3. This resulted in a decrease in sinuosity from 1.23 to 1.08 between 1833 and 1928 over the entire estuary. The trend observed in the Ems-Dollard, implies that after a period of dominant forcing by geology, autogenic processes could become more important with increased alluviation. These examples demonstrate that decreased alluviation can be associated with the stronger effects of resistant layers, because a relatively large part of the channel wetted perimeter is bounded by resistant layers. Intensified bedrock control during periods of deeper channels has also been demonstrated locally in the Marennes-Oléron Bay, France (Bertin et al., 2004). In summary, it is shown here how larger and deeper channels can trigger bedrock effects on the scale of an entire estuary via meander propagation trends. In the case of the Ems-Dollard estuary, the initial increase in channel volume and subsequent decrease over the last two centuries was not the result of changing boundary conditions. Instead, it can be linked to initial estuary expansion after storm surges in response to human-induced peatland subsidence, followed by silting up enhanced by phases of embankment (Van Maren et al., 2016; Vos & Knol, 2015).

Although channel volume and hence tidal energy in the system has varied over time, this did not seem to have strongly affected the degree to which the resistant layers could be eroded. Many Pleistocene layers did not experience significant erosion over the last centuries, despite long exposure at the channel floor. This was also observed by Schaumann et al. (2021) in a tidal channel near the German Wadden island of Norderney. The less compact and thinner Holocene peat and clays eroded faster and show clear signs of local erosion (scouring) as soon as channels form or deepened in 19th century.

5.3 | Implications for other estuaries

This study demonstrates that inherited resistant layers force the long-term morphological evolution of Holocene

20554877, 2023, 2, Downloaded from https://onlinelibrary.wiley.com/doi/10.1002/dep2.184 by Utrecht University Library, Wiley Online Library on [13/09/2023]. See the Terms and Conditions (https://onlinelibrary.wiley.com/terms-and-conditions) on Wiley Online Library for rules of use; OA articles are governed by the applicable Creative Commons License

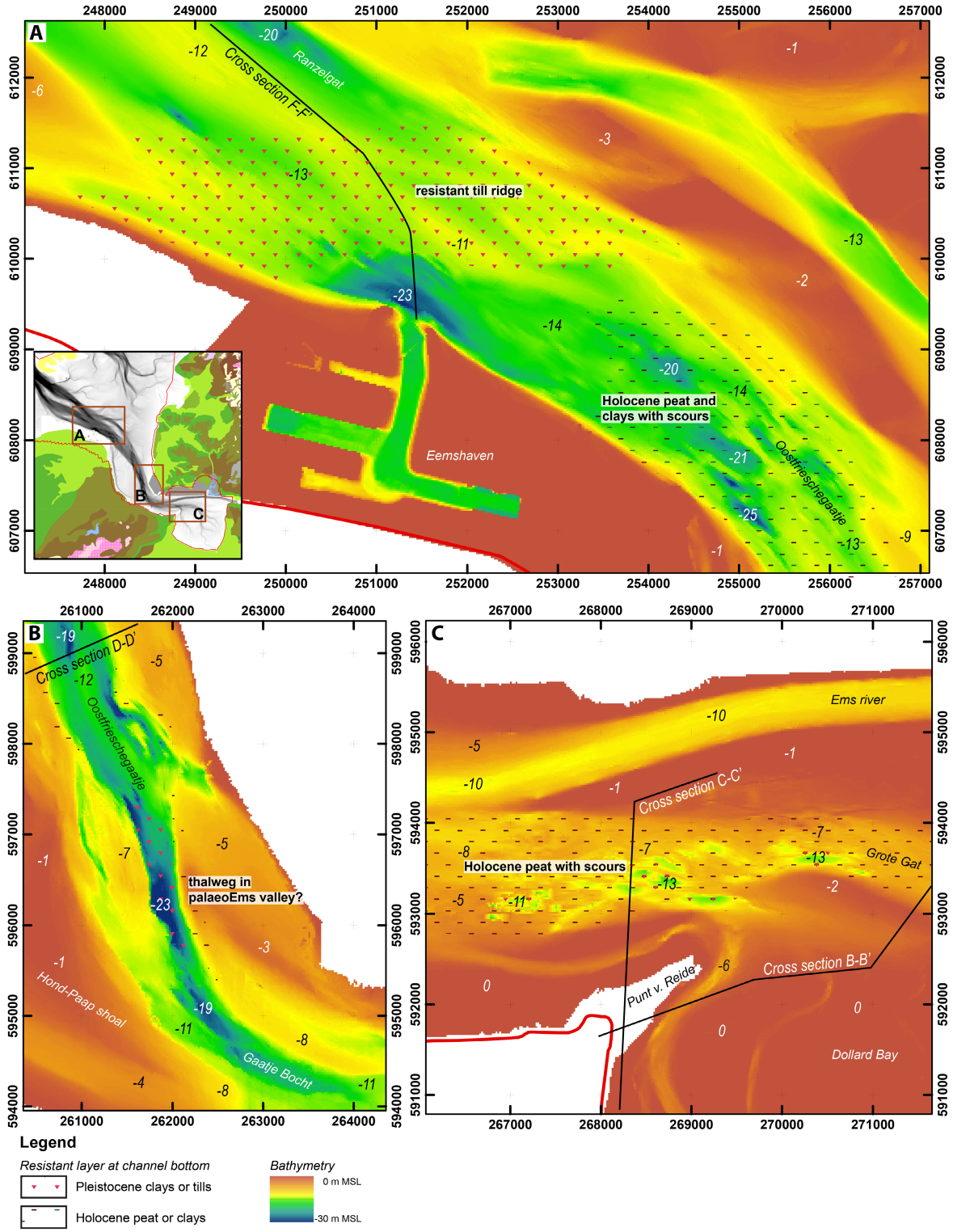

FIGURE 9 Effect of Holocene resistant layers. Bathymetry (A) 2014 (B and C) 1985 showing relatively local scour effects of Holocene resistant layers exposed at the channel bottom. Here channels have widened over the last two centuries (see Figure 7) and the peat and clay layers became exposed. For legend of the geological map in the inset, see Figure 1. Projection in Dutch coordinate system RD New (EPSG: 28992)

estuaries that were hitherto assumed to be fully alluviated (i.e. embedded in easily erodible substrate). The Ems-Dollard case illustrates how these locally present layers can affect the channel-bar pattern and planform shape of an entire estuary: they force channel, bar and node positions. These results suggest that estuary-scale forcing is

20554877, 2023, 2, Downloaded from https://onlinelibrary.wiley.com/doi/10.1002/dep2.184 by Utrecht University Library, Wiley Online Library on [13/09/2023]. See the Terms and Conditions (https://onlinelibrary.wiley.com/terms-and-conditions) on Wiley Online Library for rules of use; OA articles are governed by the applicable Creative Commons License

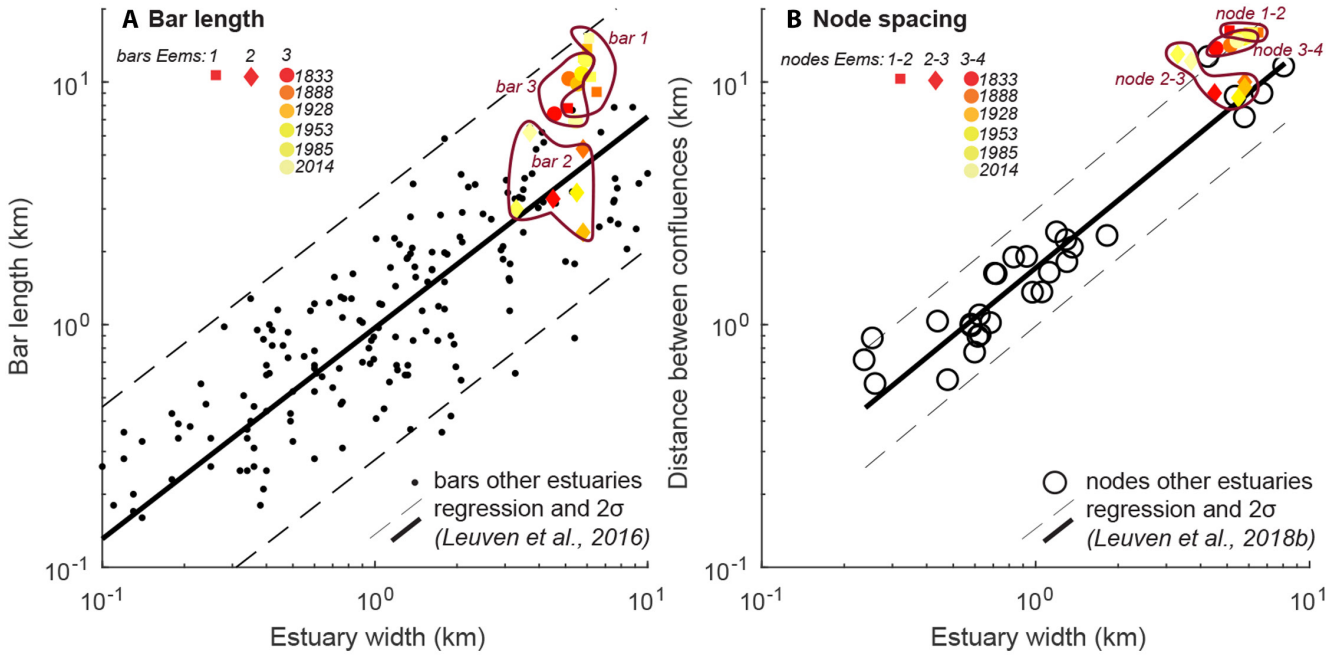

FIGURE 10 Comparison of the distance between the Ems-Dollard and other estuaries for bar length (A) and node (i.e. channel confluence) spacing (B). Reference dataset for natural bars (Leuven et al., 2016) and nodes (Leuven et al., 2018b), the latter taken from Dovey (UK), Bannow (Ireland), TawTorridge (UK), Teign (UK), Rodds Bay (Australia), Whitehaven beach (Australia) and Netarts (USA). For these estuaries, no large-scale effects of resistant layers are known. Width is measured between the outer banks of the channels. Dimensions for the Ems-Dollard were cut off at −3 m MSL, bar and node numbers in Figure 8. Solid lines indicate regression between bar length, node spacing and estuary width, dashed lines the 95% confidence limits (Leuven et al., 2016, 2018b). Bar length and node spacing is relatively high compared to reference datasets. Bar and nodes in the middle of the estuary show most complex behaviour

strongest for the cases where the spacing of independently formed inherited resistant layers is coincidently close to the hydromorphologically expected spacing between nodes in the channel-bar system.

An inventory of 27 river mouths from around the world, for which geological and bathymetrical data were available, shows that various types of resistant layers interfere with channels (in 23 out of 27 cases, values are below 1 in Figure 11), regardless of the size of the estuary and the tidal range (for sources, see Supporting Information, Table S2.1). Channel depth and the position of geological layers may vary along the estuary; here the maximum channel depths are compared to the highest position of a nearby resistant layer. This means that the resistant layers are at least locally very close to the channel floor and may potentially outcrop in many other estuaries. As such hydrodynamics and morphology may be at least locally constrained in depth, with potential estuary-wide effects as observed in the Ems-Dollard estuary. This indicates that the influence of resistant layers is most likely much more widespread than hitherto thought. This limits the applicability of concepts and models that assume full alluviation.

With increased dredging and future sea-level rise, resistant layers are expected to become more exposed at the bases and edges of channels (i.e. data points will shift down in Figure 11), increasing their potential effects on the estuary morphodynamics. Such effects are especially expected in a large number of estuaries where the tidal prism is expected to increase. This could, for example, occur when the estuary surface area becomes larger when the surrounding land drowns, when tidal amplitude at the mouth increases due to seaward shifting of amphidromic points related to sea-level changes (Idier et al., 2017; Pickering et al., 2017), or due to local anthropogenic effects (Cox et al., 2021; Huismans et al., 2021). It is well-known that increasing tidal prisms lead to channel deepening (Jarrett, 1976); and over the last 20 years already, the German Wadden Sea has shown an increase in channel volume in response to sea-level rise (Benninghoff & Winter, 2019). While deepening, resistant layers could be encountered, that potentially limit further deepening, which results in unexpected widening and subsequent land loss of the often densely populated fringing lands. In addition, where Holocene peat and clays cover the bottom of a channel, scours may form and grow as channel volume increases. These may undercut structures or channel edges, potentially causing bank instability, more than already expected from the enlargement of channel volume due to sea-level rise (Leuven et al., 2019). The filling tendency of the Ems estuary studied here suggests that such a trend can be mitigated by sediment supply.

20554877, 2023, 2, Downloaded from https://onlinelibrary.wiley.com/doi/10.1002/dep2.184 by Utrecht University Library, Wiley Online Library on [13/09/2023]. See the Terms and Conditions (https://onlinelibrary.wiley.com/terms-and-conditions) on Wiley Online Library for rules of use; OA articles are governed by the applicable Creative Commons License

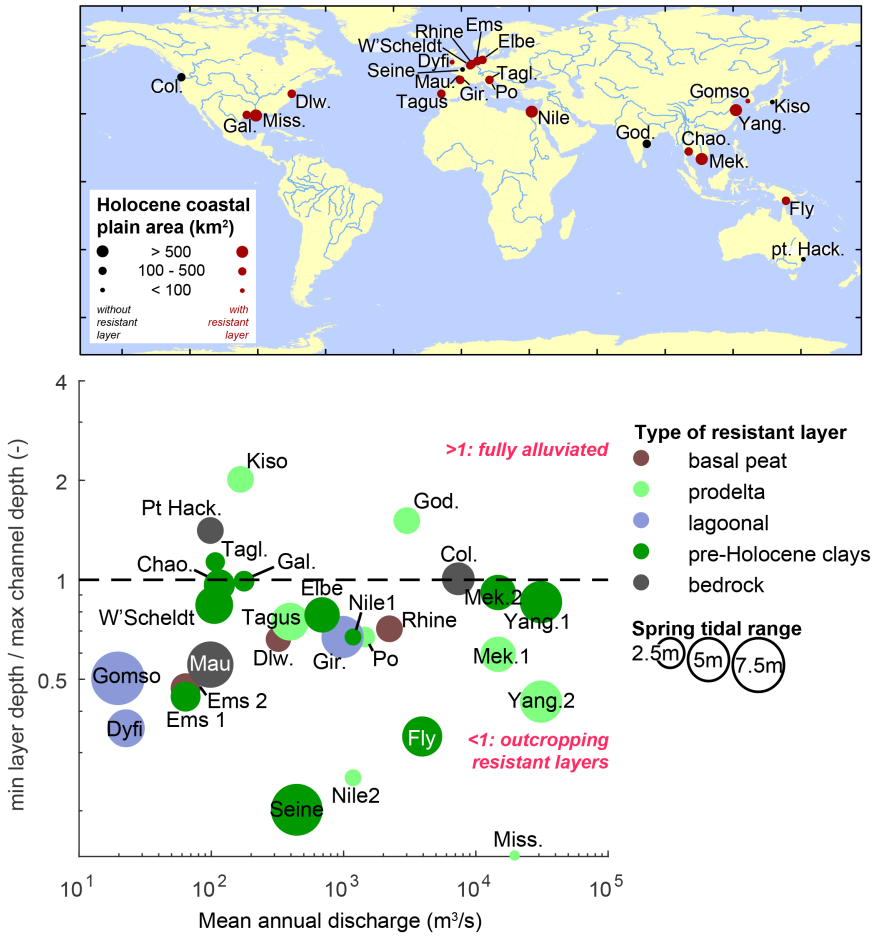

FIGURE 11 Degree of alluviation of estuaries and tidal channels in deltas worldwide, calculated as the ratio between the minimum resistant layer depth and the maximum channel depth (both below sea level). Estuaries were selected based on the availability of both bathymetric and geological cross-sections at specific positions in these estuaries, and excluded narrow laterally confined bedrock-bounded valleys. Values below 1 indicate that the vertical position of a resistant layer is higher than the deepest part of the channel close to the resistant layer. Because both channel depth and layer position may vary spatially, this does not necessarily indicate channel incision into a resistant layer. Instead, it indicates that the resistant layer may outcrop on the channel floor or is currently very close, and that, given the dynamic nature of channels, past or future exposure is likely possible. Most systems over the world have resistant layers close to their channel bases that potentially affect estuarine morphodynamics. Resistant layers are potentially relevant for all types of estuaries, independent of the size and boundary conditions (mean annual discharge and spring tidal range). For data and references, see Supporting Information, Table S2.1

Given the potential implications of resistant layers, these results highlight the need to better map shallow resistant layers in other estuaries as well. Incorporating these into morphological studies and new conceptual models would lead to improved model forecasting reliability for estuaries worldwide.

6 | CONCLUSIONS

In this paper newly compiled historical bathymetry and geological datasets are used to reconstruct the impact of resistant layers on channel-bar evolution over the last two centuries in the Ems-Dollard estuary, the Netherlands/Germany. Findings are as follows:

- The configuration of the most resistant (Pleistocene) clay layers under the Ems-Dollard estuary is the result of glacial and glaciofluvial processes, overprinted by (meltwater) valley erosion. Over the past 150 kyr, the old Ems valley has had different orientations, causing complex erosion patterns of the Pleistocene layers. The youngest Late-Weichselian Ems valley created the depocenter where Mid Holocene peat and clay are nowadays deepest and therefore most compact and erosion-resistant.
- In the Ems-Dollard estuary, channel dimensions and bar-node positions strongly depend on the presence and position of the Pleistocene resistant layers (i.e. tills and glaciolacustrine clays) in the subsurface. Depth-limiting layers force channel widening preferentially leading to

20554877, 2023, 2, Downloaded from https://onlinelibrary.wiley.com/doi/10.1002/dep2.184 by Utrecht University Library, Wiley Online Library on [13/09/2023]. See the Terms and Conditions (https://onlinelibrary.wiley.com/terms-and-conditions) on Wiley Online Library for rules of use; OA articles are governed by the applicable Creative Commons License

bar formation, while absence of resistant layers facilitates nodes.
- Effects of increased bend curvature may propagate to the adjacent bends, affecting channel-bar patterns in the entire estuary.
- Holocene resistant layers in the study area (compacted peat and tidal clays) cause scouring and edge formation on the channel floor as significant local effects.
- Both local and estuary-wide effects of resistant layers in the substrate will be larger if more of them are exposed when channel volume is increasing, for example as a result of dredging, sea-level changes or changing tidal prism. In this case this is exemplified by a stronger resistant layer effect under higher channel volumes. These were caused by human-induced land losses in the fringing peatlands, increasing tidal prism, while other boundary conditions remained relatively constant.
- Resistant layers presently seem close to the channel floor in many estuaries around the world. These may cause local effects such as unexpected widening or bank failure of usually populated estuary banks or loss of vital habitats in and along the estuary. To improve the prediction of morphological behaviour of estuaries in response to global change and human impact, resistant layers in estuaries need to be more extensively mapped and included in conceptual and numerical models.

ACKNOWLEDGEMENTS

This research was funded by Rijkswaterstaat (Eems Dollard 2050 project nr. 31126483 to MGK) and the Dutch Technology Foundation TTW, which is part of the Netherlands Organisation for Scientific Research (NWO) (grant Vici 016.140.316/13710 to MGK). The authors thank Wouter Iedema (Rijkswaterstaat), Charlotte Schmidt (Rijkswaterstaat), Bas van Maren (Deltares), Petra Dankers (RHDHV), Ad van der Spek (Deltares) and Jelmer Cleveringa (Arcadis) for discussions, and Menne Kosian (Cultural Heritage Agency), Marco van Egmond (Library Utrecht University) and Albert Oost (Deltares) for the historical maps. They thank John Shaw, Friederieke Bungenstock and Hannah Glover for their insightful reviews.

CONFLICTS OF INTEREST

The authors declare no conflict of interest.

DATA AVAILABILITY STATEMENT

The source data underlying the figures are provided as a Source Data file. The datasets generated and analysed in this study are available in the EASY DANS repository, Pierik et al. (2018): https://doi.org/10.17026/dans-x8w-wzsj

ORCID

Harm Jan Pierik https://orcid.org/0000-0001-8727-1564

REFERENCES

Allison, M.A., Dallon Weathers, H. & Meselhe, E.A. (2017) Bottom morphology in the Song Hau distributary channel, Mekong River Delta, Vietnam. *Continental Shelf Research*, *147*, 51–61.

Barckhausen, J. (1984) *Geologische Karte von Niedersachsen 1:25000, Erl. Blatt 2609*. Hannover, 109 p.

Barckhausen, J. & Streif, H. (1978) *Geologische Karte Niedersachsen 1:25000, Erl. Blatt 2608 Emden West*. Hannover, 80 p.

Behre, K.-E. (1999) *Die Veränderung der niedersächsischen Küstenlinien in den letzten 3000 Jahren und ihre Ursachen. Probleme der Küstenforschung in südlichen Nordseegebiet, 26*. Isensee Verlag, pp. 9–33.

Behre, K.-E. (2004) Coastal development, sea-level change and settlement history during the later Holocene in the Clay District of Lower Saxony (Niedersachsen), northern Germany. *Quaternary International*, *112*, 37–53.

Benninghoff, M. & Winter, C. (2019) Recent morphologic evolution of the German Wadden Sea. *Scientific Reports*, *9*, 9293.

Bertin, X., Chaumillon, E., Weber, N. & Tesson, M. (2004) Morphological evolution and time-varying bedrock control of main channel at a mixed energy tidal inlet: Maumusson Inlet, France. *Marine Geology*, *204*, 187–202.

Bouma, H., de Jong, D., Twisk, F. & Wolfstein, K. (2005) A Dutch Ecotope system for coastal waters (ZES. 1), To map the potential occurence of ecological communities in Dutch coastal and transitional waters.

Braat, L., van Kessel, T., Leuven, J.R. & Kleinhans, M.G. (2017) Effects of mud supply on large-scale estuary morphology and development over centuries to millennia. *Earth Surface Dynamics*, *5*(4), 617–652.

Brückner, M.Z., Braat, L., Schwarz, C. & Kleinhans, M.G. (2020) What came first, mud or biostabilizers? Elucidating interacting effects in a coupled model of mud, saltmarsh, microphytobenthos, and estuarine morphology. *Water Resources Research*, *56*(9), e2019WR026945.

Burningham, H. (2008) Contrasting geomorphic response to structural control: the Loughros estuaries, northwest Ireland. *Geomorphology*, *97*, 300–320.

Candel, J.H., Makaske, B., Kijm, N., Kleinhans, M.G., Storms, J.E. & Wallinga, J. (2020) Self-constraining of low-energy rivers explains low channel mobility and tortuous planforms. *The Depositional Record*, *6*(3), 648–669.

Chen, Y., Dong, J., Xiao, X., Zhang, M., Tian, B., Zhou, Y., Li, B. & Ma, Z. (2016) Land claim and loss of tidal flats in the Yangtze Estuary. *Scientific Reports*, *6*, 24018.

Coco, G., Zhou, Z., van Maanen, B., Olabarrieta, M., Tinoco, R. & Townend, I. (2013) Morphodynamics of tidal networks: advances and challenges. *Marine Geology*, *346*, 1–16.

Cox, J.R., Huismans, Y., Knaake, S.M., Leuven, J.R.F.W., Vellinga, N.E., Vegt, M., Hoitink, A.J.F. & Kleinhans, M.G. (2021) Anthropogenic effects on the contemporary sediment budget of the lower Rhine-Meuse Delta Channel Network. *Earth's Future*, *9*(7), e2020ef001869. https://doi.org/10.1029/2020ef001869

20554877, 2023, 2, Downloaded from https://onlinelibrary.wiley.com/doi/10.1002/dep2.184 by Utrecht University Library, Wiley Online Library on [13/09/2023]. See the Terms and Conditions (https://onlinelibrary.wiley.com/terms-and-conditions) on Wiley Online Library for rules of use; OA articles are governed by the applicable Creative Commons License

Dalrymple, R.W., Zaitlin, B.A. & Boyd, R. (1992) Estuarine facies models: conceptual basis and stratigraphic implications: perspective. *Journal of Sedimentary Research 62* (6), 1130–1146.

Dam, G., Van Der Wegen, M., Labeur, R.J. & Roelvink, D. (2016) Modeling centuries of estuarine morphodynamics in the Western Scheldt estuary. *Geophysical Research Letters*, *43*, 3839–3847.

De Haas, T., Pierik, H.J., van der Spek, A., Cohen, K.M., van Maanen, B. & Kleinhans, M.G. (2018) Holocene evolution of tidal systems in The Netherlands: effects of rivers, coastal boundary conditions, eco-engineering species, inherited relief and human interference. *Earth-Science Reviews*, *177*, 139–163.

De Smet, L.A.H. (1962) *Het Dollardgebied, bodemkundige en landbouwkundige onderzoekingen in het kader van de bodemkartering*. Den Haag: De Bodemkartering van Nederland, Verslagen Landbouwkundig Onderzoek.

De Vriend, H.J., Wang, Z.B., Ysebaert, T., Herman, P.M. & Ding, P. (2011) Eco-morphological problems in 183 the Yangtze Estuary and the Western Scheldt. *Wetlands*, *31*, 1033–1042.

Esselink, P., Bos, D., Oost, A.P., Dijkema, K.S., Bakker, R. & de Jong, R. (2011). Exploration of erosion of the marshes in the Ems–Dollard. PUCCIMAR Rapport 02, A&W Rapport 1574.

Essink, K. (1999) Ecological effects of dumping of dredged sediments; Options for management. *Journal of Coastal Conservation*, *5*, 69–80.

Ey, J. (2010) Initiation of dike-construction in the German clay district. *Wadden Sea Ecosystem*, *26*, 179–183.

Fagherazzi, S. & Furbish, D.J. (2001) On the shape and widening of salt marsh creeks. *Journal of Geophysical Research: Ocean*, *106*, 991–1003.

Fitzgerald, D.M., Buynevich, I.V., Fenster, M.S. & McKinlay, P.A. (2000) Sandy dynamics at the mouth of a rock-bound, tide-dominated estuary. *Sedimentary Geology*, *131*, 25–49.

Gerritsen, F. (1952) *Historical and hydrographical investigations in the Ems estuary* (in Dutch). Hoorn: Ministry of Public Works, Report D41. http://publicaties.minienm.nl/documenten/historisch-hydrografisch-onderzoek-eems [Accessed on 18th March 2019].

Gruijters, S.H.L.L., Schokker, J. & Veldkamp, J.G. (2004) Kartering moeilijk erodeerbare lagen in het Schelde estuarium. NITG Report, 213 p.

Gunnink, J.L., Maljers, D., Gessel, S.F.V., Menkovic, A. & Hummelman, H.J. (2013) Digital Geological Model (DGM): a 3D raster model of the subsurface of the Netherlands. *Netherlands Journal of Geosciences*, *92*(1), 33–46.

Heap, A.D. & Nichol, S.L. (1997) The influence of limited accommodation space on the stratigraphy of an incised-valley succession: Weiti River estuary, New Zealand. *Marine Geology*, *144*, 229–252.

Hepp, D.A., Romero, O.E., Mörz, T., de Pol-Holz, R. & Hebbeln, D. (2019) How a river submerges into the sea: a geological record of changing a fluvial to a marine paleoenvironment during early Holocene sea level rise. *Journal of Quaternary Science*, *34*, 581–592.

Herrling, G. & Niemeyer, H.D. (2008) *Comparison of the hydrodynamic regime of 1937 and 2005 in the Ems-Dollard estuary by applying mathematical modeling*. Norden: HARBASINS Report: NLWKN Coastal Research Station.

Hibma, A., Schuttelaars, H.M. & De Vriend, H.J. (2004) Initial formation and long-term evolution of channel-shoal patterns. *Continental Shelf Research*, *24*, 1637–1650.

Hijma, M.P. (2016) Geology of the Dutch coast: The effect of lithological variation on coastal morphodynamics. Deltares report, 47.

Hoitink, A.J.F., Wang, Z.B., Vermeulen, B., Huismans, Y. & Kästner, K. (2017) Tidal controls on river delta morphology. *Nature Geoscience*, *10*, 637–645.

Homeier, H. (1962) Historisches Kartenwerk 1:50 000 der niedersächsischen Küste, Jahresbericht der Forschungsstelle Küste, Band XIII.

Homeier, H. (1977) Einbruch und weitere Entwicklung des Dollart bis um 1600, Jahresbericht 1976 der Forschungsstelle für Insel- und Küstenschutz der Niedersächsischen Wasserwirtschaftsverwaltung. Nordeney 39–81 & B2 Anlage 1–16.

Huismans, Y., Koopmans, H., Wiersma, A., de Haas, T., Berends, K., Sloff, K. & Stouthamer, E. (2021) Lithological control on scour hole formation in the Rhine-Meuse Estuary. *Geomorphology*, *385*, 107720.

Huismans, Y., van Velzen, G., O'Mahoney, T.S.D., Hoffmans, G. & Wiersma, A.P. (2016) Scour hole development in river beds with mixed sand-clay-peat stratigraphy. Scour and Erosion—Proceedings of 8th International Conference on Scour and Erosion, ICSE 2016, 801–807.

Huuse, M. & Lykke-Andersen, H. (2000) Overdeepened Quaternary valleys in the eastern Danish North Sea: morphology and origin. *Quaternary Science Reviews*, *19*, 1233–1253.

Idier, D., Paris, F., Le Cozannet, G., Boulahya, F. & Dumas, F. (2017) Sea-level rise impacts on the tides of the European shelf. *Continental Shelf Research*, *137*, 56–71.

Jarrett, J.T. (1976) Tidal prism – inlet area relationships, 32 p.

Jonkman, H. & De Vries, K. (2010) Bodemopbouw vaarweg Eemshaven-Noordzee, Medusa report.

Kirwan, M.L. & Megonigal, J.P. (2013) Tidal wetland stability in the face of human impacts and sea-level rise. *Nature*, *504*, 53–60.

Kleinhans, M.G., Douma, H., Addink, E.A., Coumou, L., Deggeller, T., Jentink, R., Paree, E. & Cleveringa, J. (2021) Salt marsh and tidal flat area distributions along three estuaries. *Frontiers in Marine Science*, *8*, 1503.

Kruiver, P.P., Wiersma, A., Kloosterman, F.H., de Lange, G., Korff, M., Stafleu, J., Busschers, F.S., Harting, R., Gunnink, J.L., Green, R.A., van Elk, J. & Doornhof, D. (2017) Characterisation of the Groningen subsurface for seismic hazard and risk modelling. *Netherlands Journal of Geosciences*, *96*, s215–s233.

Leuven, J.R.F.W., Braat, L., van Dijk, W.M., de Haas, T., van Onselen, E.P., Ruessink, B.G. & Kleinhans, M.G. (2018b) Growing Forced Bars Determine Nonideal Estuary Planform. *Journal of Geophysical Research: Earth Surface*, *123*(11), 2971–2992. https://doi.org/10.1029/2018JF004718

Leuven, J.R.F.W., de Haas, T., Braat, L. & Kleinhans, M.G. (2018c) Topographic forcing of tidal sandbar patterns for irregular estuary planforms. *Earth Surface Processes and Landforms*, *43*, 172–186.

Leuven, J.R.F.W., Kleinhans, M.G., Weisscher, S.A.H. & van der Vegt, M. (2016) Tidal sand bar dimensions and shapes in estuaries. *Earth-Science Reviews*, *161*, 204–223.

Leuven, J.R.F.W., Pierik, H.J., van der Vegt, M., Bouma, T.J. & Kleinhans, M.G. (2019) Sea-level-rise-induced threats depend on the size of tide-influenced estuaries worldwide. *Nature Climate Change*, *9*(12), 986–992.

Leuven, J., Verhoeve, S., van Dijk, W., Selaković, S. & Kleinhans, M. (2018a) Empirical assessment tool for bathymetry, flow velocity

20554877, 2023, 2, Downloaded from https://onlinelibrary.wiley.com/doi/10.1002/dep2.184 by Utrecht University Library, Wiley Online Library on [13/09/2023]. See the Terms and Conditions (https://onlinelibrary.wiley.com/terms-and-conditions) on Wiley Online Library for rules of use; OA articles are governed by the applicable Creative Commons License

and salinity in estuaries based on tidal amplitude and remotely-sensed imagery. *Remote Sensing*, *10*, 1915.

Monbaliu, J., Chen, Z., Felts, D., Ge, J., Hissel, F., Kappenberg, J., Narayan, S., Nicholls, R.J., Ohle, N., Schuster, D., Sothmann, J. & Willems, P. (2014) Risk assessment of estuaries under climate change: lessons from Western Europe. *Coastal Engineering*, *87*, 32–49.

Mosselman, E., Shishikura, T. & Klaassen, G.J. (2000) Effect of bank stabilization on bend scour in anabranches of braided rivers. *Physics and Chemistry of the Earth, Part B: Hydrology, Oceans and Atmosphere*, *25*, 699–704.

Mulder, H.P.J. (2013) Dredging Volumes in the Ems–Dollard Estuary for the Period 1960–2011.

Nicholls, R.J. & Cazenave, A. (2010) Sea-level rise and its impact on coastal zones (June, pg 1517, 2007). *Science (80-.)*. *329*, 628.

Nittrouer, J.A., Mohrig, D., Allison, M.A. & Peyret, A.P.B. (2011) The lowermost Mississippi River: a mixed bedrock-alluvial channel. *Sedimentology*, *58*, 1914–1934.

Oberrecht, D., Franz, B. & Wurpts, A. (2016) Hydro- und morphodynamische Auswirkungen eines Tidesteuerungsbetriebes mit dem Emssperrwerk.

Oost, A.P. (1995) *Dynamics and Sedimentary Development of the Dutch Wadden Sea with Emphasis on the Frisian Inlet*. PhD Thesis, Utrecht, Utrecht University.

Pickering, M.D., Horsburgh, K.J., Blundell, J.R., Hirschi, J.J., Nicholls, R.J., Verlaan, M. & Wells, N.C. (2017) The impact of future sea-level rise on the global tides. *Continental Shelf Research*, *142*, 50–68.

Pierik, H.J. (2010) *An integrated approach to reconstruct the Saalian glaciation*. MSc thesis, Utrecht University, 142 p.

Pierik, H.J., Busschers, F.S., van Egmond, M., Kosian, M.C. & Kleinhans, M.G. (2018) GIS dataset historical bathymetry and resistant layers in the Ems-Dollard estuary/Toelichting GIS dataset historische bathymetrie en resistente lagen Eems-Dollard.

Pierik, H.J., Cohen, K.M., Vos, P.C., Van der Spek, A.J.F. & Stouthamer, E. (2017) Late Holocene coastal-plain evolution of the Netherlands: the role of natural preconditions in human-induced sea ingressions. *Proceedings of the Geologists' Association*, *128*(2), 180–197.

Praeg, D. (2003) Seismic imaging of mid-Pleistocene tunnel-valleys in the North Sea Basin—high resolution from low frequencies. *Journal of Applied Geophysics*, *53*(4), 273–298.

Ralston, D.K. & Geyer, W.R. (2009) Episodic and long-term sediment transport capacity in the Hudson River estuary. *Estuaries and Coasts*, *32*, 1130.

Rappol, M. (1987) Saalian till in The Netherlands: a review. In: van der Meer, J.J.M. (Ed.) *Tills and glaciotectonics*. Rotterdam: Balkema, pp. 3–21.

Roeleveld, W. (1974) The Holocene Evolution of the Groningen Marine-Clay District. *Ber. van Rijksd. voor het Oudheidkd. Bodemonderz*, *24*, 1–133.

Savenije, H.H.G. (2015) Prediction in ungauged estuaries: An integrated theory. *Water Resources Research*, *51*, 2464–2476.

Schaumann, R.M., Capperucci, R.M., Bungenstock, F., McCann, T., Enters, D., Wehrmann, A. & Bartholomä, A. (2021) The Middle Pleistocene to early Holocene subsurface geology of the Norderney tidal basin: new insights from core data and high-resolution sub-bottom profiling (Central Wadden Sea, southern North Sea). *Netherlands Journal of Geosciences*, *100*.

Sloff, K., Van Spijk, A., Stouthamer, E. & Sieben, A. (2013) Understanding and managing the morphology of branches incising into sand-clay deposits in the Dutch Rhine Delta. *International Journal of Sedimentary Research*, *28*, 127–138.

Stratingh, G.A. & Venema, G.A. (1855) De Dollard of Geschied-, Aardrijksen Natuurkundige beschrijving van dezen Boezem der Eems. Groningen, XVI.

Streif, H. (2004) Sedimentary record of Pleistocene and Holocene marine inundations along the North Sea coast of Lower Saxony, Germany. *Quaternary International*, *112*, 3–28.

TNO-GSN. (2021a) TNO - Geological Survey of the Netherlands. Digital Geological Model (DGM; Gunnink et al., 2013) v2.2 and GeoTOP model v1.4. Available at: https://www.dinoloket.nl/ondergrondmodellen [Accessed on 1st June 2021].

TNO-GSN. (2021b) TNO - Geological Survey of the Netherlands. Stratigrafische Nomenclator van Nederland. Available at: http://www.dinoloket.nl/stratigrafische-nomenclator/ [Accessed on 1st June 2021].

Townend, I. (2012) The estimation of estuary dimensions using a simplified form model and the exogenous controls. *Earth Surface Processes and Landforms*, *37*, 1573–1583.

Van de Lageweg, W.I., Braat, L., Parsons, D.R. & Kleinhans, M.G. (2018) Controls on mud distribution and architecture along the fluvial-to-marine transition. *Geology*, *46*(11), 971–974.

Van den Berg, M.W. & Beets, D.J. (1987) Saalian glacial deposits and morphology in The Netherlands. In: van der Meer, J.J.M. (Ed.) *Tills and glaciotectonics*. Rotterdam: Balkema, pp. 235–251.

Van der Wegen, M. (2013) Numerical modeling of the impact of sea level rise on tidal basin morphodynamics. *Journal of Geophysical Research: Earth Surface*, *118*, 447–460.

Van der Wegen, M. & Roelvink, J.A. (2012) Reproduction of estuarine bathymetry by means of a process-based model: Western Scheldt case study, the Netherlands. *Geomorphology*, *179*, 152–167.

Van Dijk, W.M., Cox, J.R., Leuven, J.R.F.W., Cleveringa, J., Taal, M., Hiatt, M.R., Sonke, W., Verbeek, K., Speckmann, B. & Kleinhans, M.G. (2020) The vulnerability of tidal flats and multi-channel estuaries to dredging and disposal. *Anthropocene Coasts*, *4*(1), 36–60.

Van Dijk, W.M., Van De Lageweg, W.I. & Kleinhans, M.G. (2012) Experimental meandering river with chute cutoffs. *Journal of Geophysical Research: Earth Surface*, *117*, 1–18.

Van Maren, D.S., Oost, A.P., Wang, Z.B. & Vos, P.C. (2016) The effect of land reclamations and sediment extraction on the suspended sediment concentration in the Ems Estuary. *Marine Geology*, *376*, 147–157.

Van Maren, D.S., Van Kessel, T., Cronin, K. & Sittoni, L. (2015) The impact of channel deepening and dredging on estuarine sediment concentration. *Continental Shelf Research*, *95*, 1–14.

Van Veen, J. (1950) Ebb-and flood-channel systems in the Dutch tidal waters. *Tijdschr van het Aardrijkskd Genoot*, *67*(3), 303–325.

Van Veen, J., Van der Spek, A.J., Stive, M.J. & Zitman, T. (2005) Ebb and flood channel systems in the Netherlands tidal waters. *Journal of Coastal Research*, *21*(6), 1107–1120. https://doi.org/10.2112/04-0394.1

Van Wesenbeeck, B.K., Mulder, J.P.M., Marchand, M., Reed, D.J., de Vries, M.B., de Vriend, H.J. & Herman, P.M.J. (2014) Estuarine, Coastal and Shelf Science Damming deltas: a practice of the past? Towards nature-based flood defenses. *Estuarine, Coastal and Shelf Science*, *140*, 1–6.

20554877, 2023, 2, Downloaded from https://onlinelibrary.wiley.com/doi/10.1002/dep2.184 by Utrecht University Library, Wiley Online Library on [13/09/2023]. See the Terms and Conditions (https://onlinelibrary.wiley.com/terms-and-conditions) on Wiley Online Library for rules of use; OA articles are governed by the applicable Creative Commons License

Vos, P.C. & Bungenstock, F. (2013) Abriss der Landschafts- und Küstenentwicklung/Schets van de ontwikkeling van het kustlandschap. In: Kegler, J.F. (Ed.) *Land der Entdeckungen. Die Archäologie des friesischen Küstenraums*. Aurich: Ostfriesische Landschaft, pp. 60–69.

Vos, P.C. & Knol, E. (2015) Holocene landscape reconstruction of the Wadden Sea area between Marsdiep and Weser. *Netherlands Journal of Geoscience*, *94*, 157–183.

Vos, P.C. & Van Kesteren, W.P. (2000) The long-term evolution of intertidal mud flats in the northern Netherlands during the Holocene; natural and anthropogenic processes. *Continental Shelf Research*, *20*, 31–38.

Wang, S., Fu, B., Piao, S., Lü, Y., Ciais, P., Feng, X. & Wang, Y. (2016) Reduced sediment transport in the Yellow River due to anthropogenic changes. *Nature Geoscience*, *9*, 38–41.

Wilson, C., Goodbred, S., Small, C., Gilligan, J., Sams, S., Mallick, B. & Hale, R. (2017) Widespread infilling of tidal channels and navigable waterways in human-modified tidal deltaplain of southwest Bangladesh. *Elementa: Science of the Anthropocene*, *5*, 78.

SUPPORTING INFORMATION

Additional supporting information may be found in the online version of the article at the publisher's website.

How to cite this article: Pierik, H.J., Leuven, J.R.F.W., Busschers, F.S., Hijma, M.P. & Kleinhans, M.G. (2023) Depth-limiting resistant layers restrict dimensions and positions of estuarine channels and bars. *The Depositional Record*, 9, 213–232. Available from: https://doi.org/10.1002/dep2.184

20554877, 2023, 2, Downloaded from https://onlinelibrary.wiley.com/doi/10.1002/dep2.184 by Utrecht University Library, Wiley Online Library on [13/09/2023]. See the Terms and Conditions (https://onlinelibrary.wiley.com/terms-and-conditions) on Wiley Online Library for rules of use; OA articles are governed by the applicable Creative Commons License